Pluripotent stem cell-derived islet encapsulation in alginate beads via a scalable emulsion-based process

Arianna Castro Rojas

Department of Bioengineering & Department of Biomedical Engineering

McGill University, Montreal

Montreal, Quebec, Canada

February 2025

A thesis submitted to McGill University in partial fulfillment of the requirements for the degree of Master of Engineering (MEng.)

Table of contents

List of Figures

List of Tables

Abstract

Type I diabetes (T1D) results from the autoimmune destruction of insulin-producing beta-cells in the pancreatic islets of Langerhans. While insulin therapy is common, the refined blood glucose regulation of endogenous islets remains unmatched, leading to chronic conditions such as kidney failure and amputations. Islet transplantation is an alternative to daily insulin administration, but it faces challenges such as limited donor availability and the need for lifelong immunosuppression. Pluripotent stem cell-derived islets (SC-islets) offer a potentially unlimited source for transplantation. The scale-up of extended SC-islet suspension cultures can be problematic due to cellular agglomeration and shear-induced damage. We hypothesized that alginate immobilization would enable scale-up by creating a local environment that would prevent agglomeration, exposure to high shear, and potentially also afford control over differentiation mechanisms.

Immature (Stage 6 of a 7-stage directed differentiation protocol starting from pluripotent stem cells) SC-islets were immobilized in different concentrations of alginate microbeads. To demonstrate scale-up potential, the encapsulation was performed in a stirred vessel through emulsification and internal gelation, and the SC-islets, with or without encapsulation, were cultured both in downscaled stirred suspension as well as in vertical wheel bioreactors. When higher concentrations of alginate were used, the fraction of beta-cells decreased while the fraction of alpha-cells increased during 25-day maturation up to Stage 7. Non-encapsulated SC-islets cultured in vertical wheel bioreactors exhibited extensive cluster fusion, resulting in a sevenfold increase in aggregate size and a significantly lower cell recovery rate (68 ± 3.8%) compared to encapsulated SC-islets (90 ± 4.9%). However, static glucose-stimulated insulin secretion (GSIS)

assays revealed that the non-immobilized SC-islets secrete more insulin (normalized by total DNA) relative to the downscaled stirred suspension. In contrast, the functionality of the encapsulated SC-islets remained comparable to non-encapsulated SC-islets. In conclusion, SC-islets can be successfully immobilized in 2% to 7% alginate beads using a scalable, cost-effective emulsion-based process. The alginate concentration plays a role in endocrine specification, likely through differences in mechanical signals. Furthermore, encapsulating SC-islets prevents islet agglomeration, resulting in higher cell recovery compared to non-encapsulated SC-islets when cultured in vertical wheel bioreactors. This work provides an avenue to scale up long-term SC-islet suspension cultures with high ease of processing and recovery rates from beads. The process could be applied to other organoid cultures that require scale-up and extended culture periods.

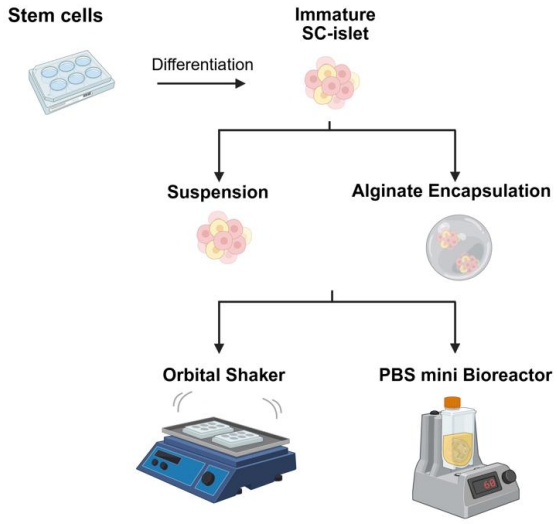

Graphical Abstract. Created with BioRender.com

Résumé

Le diabète de type I (DT1) résulte de la destruction auto-immune des cellules bêta productrices d'insuline des îlots de Langerhans du pancréas. Bien que la thérapie à l'insuline soit courante, la régulation raffinée de la glycémie par les îlots endogènes reste inégalée, ce qui conduit à des conditions chroniques telles que l'insuffisance rénale et les amputations. La transplantation d'îlots est une alternative à l'administration quotidienne d'insuline, mais elle présente des défis tels que la disponibilité limitée des donneurs et la nécessité d'une immunosuppression à vie. Les îlots dérivés de cellules souches pluripotentes (îlots-CS) offrent une source potentiellement illimitée pour la transplantation. L'augmentation de l'échelle des cultures en suspension d'îlots-CS peut être problématique en raison de l'agglomération cellulaire et des dommages induits par le cisaillement. L'hypothèse de ce projet était que l'immobilisation des îlots-CS dans l'alginate pourrait faciliter la mise à l'échelle des cultures en créant un environnement local qui empêcherait l'agglomération cellulaire, l'exposition au cisaillement élevé tout en permettant de contrôler les mécanismes de différenciation.

Les îlots-CS immatures (Stade 6 d'un protocole de différenciation dirigée en 7 étapes à partir de cellules souches pluripotentes) ont été immobilisés dans différentes concentrations de billes d'alginate. Afin de démontrer le potentiel de mise à l'échelle, l'encapsulation a été réalisée dans un récipient agité par émulsification et gélification interne. Les îlots-CS, avec ou sans encapsulation, ont été cultivés soit dans une suspension agitée à petite échelle, soit dans des bioréacteurs à roue verticale. Lorsque des concentrations plus élevées d'alginate ont été utilisées, la fraction de cellules bêta a diminué, tandis que la fraction de cellules alpha a augmenté pendant la maturation de 25 jours jusqu'au stade 7. Les îlots-CS non encapsulés cultivés dans des bioréacteurs à roue verticale ont présenté une fusion étendue des amas, entraînant une

augmentation de taille des agrégats par un facteur de sept et un taux de récupération cellulaire significativement plus faible (68 ± 3,8 %) comparé aux îlots-CS encapsulés (90 ± 4,9 %). Cependant, les tests de sécrétion d'insuline stimulée par le glucose en condition statique (GSIS) ont révélé que les îlots-CS non immobilisés sécrètent davantage d'insuline (normalisée par la quantité totale d'ADN) par rapport à ceux cultivés en suspension agitée à échelle réduite. En revanche, la fonctionnalité des îlots-CS encapsulés est restée comparable à celle observée dans les cultures non-encapsulées. En conclusion, les îlots-CS peuvent être immobilisés avec succès dans des billes d'alginate de 2 % à 7 % à l'aide d'un processus basé sur l'émulsion, un procédé peu coûteux qui peut être mis à l'échelle. La concentration en alginate joue un rôle dans la spécification endocrinienne, probablement via un changement des stimuli mécaniques. De plus, l'encapsulation des îlots-CS évite l'agglomération des îlots, ce qui entraîne une meilleure récupération cellulaire par rapport aux îlots-CS non-encapsulés lorsqu'ils sont cultivés dans des bioréacteurs à roue verticale. Ce travail pose les assises vers la mise à l'échelle des cultures en suspension à long terme d'îlots-CS avec une grande facilité de manutention et des taux de récupération élevés des billes. Le processus pourrait être appliqué à d'autres cultures d'organoïdes nécessitant la mise à l'échelle et des cultures de longue durée.

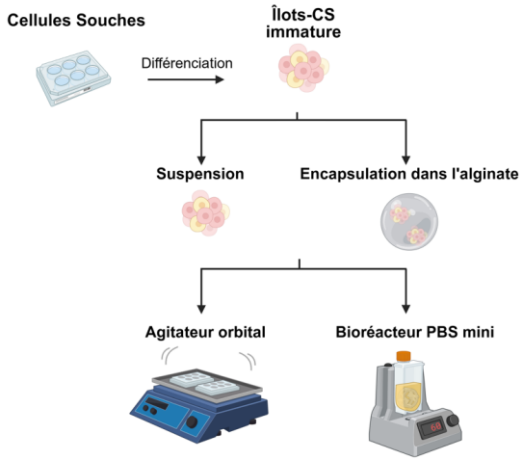

Résumé Graphique. Créé avec BioRender.com

List of abbreviations

ESCs	Embryonic stem cells
hPSCs	Human pluripotent stem cells
SC-islets	Stem cell-derived islets
S1D3	Stage 1-day 3
SD43	Stage 4-day 3
S6D7	Stage 6-day 7
S7D10	Stage 7 day-10
S7D25	Stage 7 day-25
PC2	Prohormone convertase 2
PDX1	Pancreatic and duodenal homeobox 1
GcgR	Glucagon receptor
GLP-1	Glucagon-like Peptide-1 receptoR
T1DM	Type I diabetes mellitus
DM	Diabetes mellitus
T2DM	Type II diabetes mellitus
IEQ	Islet equivalent

Acknowledgements

I would like to express my gratitude my supervisor, Dr. Corinne Hoesli, for believing in me and taking me as her student, despite my limited research experience. Thank you for your consistent support and guidance throughout all stages of this project, and for inspiring me to grow in the bioprocess engineering field.

A special thank you to Janathan Brassard for being a great mentor, and friend. Thank you for providing me your help and advice over the years. I also want to thank Florent Lemaire, Hamid Ebrahimi Orimi, and Robert Chen, for your mentoring, for always being available to offer advice, guidance, and help throughout this journey.

Thank you, Lisa Danielczak, for your constant support, giving me training in cell culture, handling all the orders, and always being there when I needed advice or help with the various lab equipment.

Thank you, Francesco Touani Kameni and Professor. Sophie Lerouge for allowing me to use the MicroSquisher (CellScale) equipment, which made it possible to perform the mechanical characterization of our microbeads.

To my mom (Ms. Doris Rojas Chaves) and dad (Mr. Oscar Castro Perez), thank you for your unconditional support and love. Thank you for backing me in every decision I've made, even when it meant moving to another country in the middle of winter. Thank you for being my safe place, for nurturing my creativity and curiosity; without you, this journey wouldn't have been possible.

Finally, I must thank every Hoesli lab member for being supportive, good friends, and making this process a great experience.

Contribution of Authors

I contributed to the initial project concept, conducted the experiments, analyzed the results, and performed the statistical analysis. I also prepared all the figures and wrote the manuscript. The experiments involved modifying the initial emulsion-based encapsulation method by adjusting various parameters to obtain beads with different alginate concentrations but similar D[4.3], ensuring high SC-islet viability. Additionally, I carried out multiple stem cell-derived pancreatic differentiations, characterized the SC-islets, assessed the mechanical properties of the beads, and conducted bioreactor cultures of SC-islets.

Jonathan Brassard contributed to the initial project idea and provided SC-islets for the analysis of aggregate size and the impact of alginate encapsulation on SC-islet differentiation outcomes (objectives 1 and 2).

Florent Lemaire assisted in modifying the emulsion-based encapsulation protocol, supported the daily feeding of the SC-islets, and helped in the analysis of the glucose-stimulated insulin secretion samples.

Hamid Ebrahimi Orimi provided SC-islets for the PBS mini bioreactor culture and supported the daily feeding of the SC-islets.

Robert Chen assisted with the lab execution of the mechanical characterization analysis of the beads.

Professor Corinne Hoesli contributed to the initial project idea, secured funding, provided mentorship, guidance and valuable insights throughout the project, and edited the thesis.

1. Introduction

Type 1 diabetes is an autoimmune disease that leads to the destruction of insulin-producing pancreatic beta cells [1]. Islet transplantation has emerged as an alternative to daily insulin injections to regulate blood glucose levels. However, limited islet sources and life-long immunosuppression required to limit graft rejection hinder its widespread application. Stem cell-derived islets (SC-islets) have emerged as a potentially unlimited cell source [2].

Devices composed of islets encapsulated in hydrogels have been used to create a physical barrier between exogenous cells and the host immune system. The barrier permits the diffusion of essential nutrients and small molecules, such as insulin and glucagon, while minimizing the risk of autoimmune response and potential transplant rejection [3,4]. Moreover, encapsulation is expected to improve the safety of SC-islets by allowing graft containment and potential retrieval if concerns arise. The three-dimensional (3D) environment created by the encapsulation may provide various mechanical stimuli that can impact the differentiation outcome [5].

The encapsulation of pluripotent stem cells (PSCs) in microbeads for bioprocess scale-up has been widely used to protect the cells from the shear-mediated damage caused by the impeller of the mixing system [6,7]. The goal of this project was to study the impact of alginate encapsulation microenvironment on the differentiation of SC-islets. Additionally, we aimed to investigate whether emulsion-based encapsulation could protect the SC-islets from agglomeration and local energy dissipation rates in the bioreactor, thereby enhancing bioprocess scale-up. We hypothesized that emulsion-based encapsulation could minimize local flow effects on SC-islets, while alginate concentration may impact their maturation.

Our results suggest that encapsulation influences the maturation of SC-islets' identity. Stiffer environments promoted glucagon-producing alpha-cell differentiation, while softer or non-encapsulated conditions favored insulin-producing beta-cell maturation. Furthermore, as a proof of concept (N=2) to assess the feasibility of SC-islet encapsulation in bioprocess scale-up, encapsulated and non-encapsulated semi-mature SC-islets were cultured 25 days in 100 mL vertical wheel bioreactors.

The goal of this project was to investigate whether alginate microencapsulation can protect SC-islets from agglomeration and local energy dissipation, while also studying the effect of the alginate microenvironment on the maturation of SC-islets. We hypothesized that alginate immobilization would enable scale-up by creating a local environment that would prevent agglomeration, and exposure to high shear. Furthermore, the stiffness of the microenvironment may have an impact on the identity and functionality of the maturing SC-islets due to mechanical stimuli, and nutrients diffusion.

2. Literature Review

2.1. Islet biology and diabetes

The pancreas is located retroperitoneally within the abdominal cavity, spanning between the L1 and L2 vertebrae. It functions as a digestive gland with both endocrine and exocrine properties [8,9]. The endocrine portion of the pancreas is comprised of pancreatic islet cells, also referred to as islets of Langerhans. The pancreatic islets are composed by several types of cells: insulin-producing beta-cells, glucagon-producing alpha-cells, somatostatin-producing delta-cells, and pancreatic polypeptides [10]. Furthermore, the exocrine portion of the pancreas is composed by acinar cells and ductal structures. The acinar cells plays a key role in the production, storage, and secretion of various enzymes involved in the food digestion and nutrients absorption [11]. Figure 1 provides a comprehensive overview of the structure of a healthy pancreas.

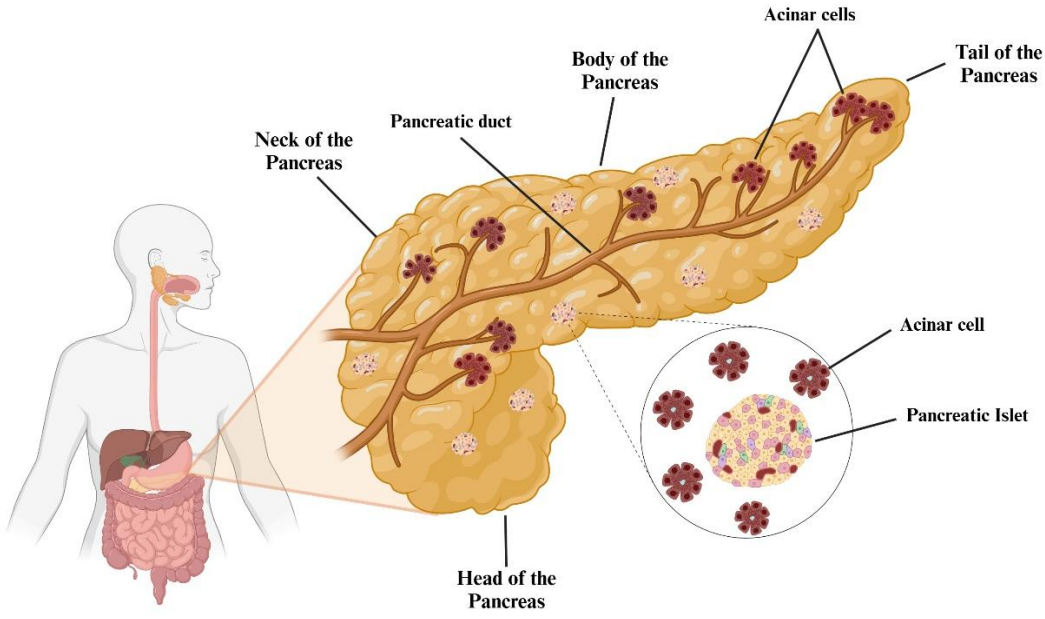

Figure 1.Structural overview of a healthy pancreas. Exocrine (pancreatic islets) and Endocrine (pancreatic duct and acinar cells) components. Created with BioRender.com

The islet of Langerhans plays a crucial role in glucose homeostasis and energy metabolism due to their secretory functions. It has been reported that the human pancreas contains approximately 1-3 million islets distributed throughout the pancreatic structure [12,13]

Pancreatic alpha-cells are responsible for secreting the hormone glucagon, which is derived from the 160-residue proglucagon peptide through the action of prohormone convertase 2 (PC2). These cells originate from the endoderm, and their differentiation requires the presence of several key transcription factors, including the homeobox protein Nkx6.1. During early stages of development, the transcription factor PDX1 plays a crucial role in pancreatic development and is expressed across the entire epithelial structure. However, in early glucagon-positive cells, the expression of PDX1 is suppressed [14–16].

Glucagon is a hormone that binds to the glucagon receptor found in various organs including liver, brain, kidney, pancreas, and smooth muscle. It plays a crucial role in protecting the body from hypoglycaemia by increasing blood glucose levels. The primary action of glucagon occurs in the liver, where it promotes gluconeogenesis and glycogenolysis. Furthermore, it's been shown that glucagon is also involved in promoting insulin secretion by interacting with the glucagon receptor (GcgR) and glucagon-like peptide-1 receptor (GLP-1) located at the surface of the beta-cells [17]. These processes help ensure an adequate supply of glucose to different organs, maintaining energy balance and preventing dangerously low blood sugar levels [16,18].

Pisania *et al.* quantified the cell fraction in the pancreas, finding that 48.3 ± 2.6% of the total pancreas consist of islet cells. Of this, 73.6% of the islet cell population is made up of insulin-producing beta-cells [19]. These pancreatic cells are the primary source of insulin in the body; they synthesize, store, and release this hormone, playing a crucial role in maintaining glucose homeostasis [20]. Insulin is a hormone composed by a heterodimeric peptide with two chains; chain

A, consisting of 21 amino acids, and chain B, made up of 30 amino acids. The chains are connected by two interpeptide disulfide bonds (CysB7 to CysA7 and CysB19 to CysA20) and an interpeptide disulfide bond (CysA6 to CysA11) [21].

2.2. Insulin secretion mechanism

Beta cells, located in the pancreatic islets, secrete the peptide hormone insulin in response to glucose stimulation. When blood glucose levels are elevated, beta cells release insulin, which facilitates glucose uptake by various tissues, including the liver, adipose tissue, and skeletal muscle [22].

The process of insulin production and secretion involves several key steps, beginning with the expression of the INS gene (1431bp) within pancreatic beta cells. After transcription and post translational modifications, the precursor molecular preproinsulin is synthesized. Preproinsulin is then converted to proinsulin in the endoplasmic reticulum (ER) [23]. Proinsulin is subsequently packaged into secretory granules in the Golgi apparatus, where it undergoes further maturation to yield mature insulin and C-peptide in a 1:1 ratio. The mature insulin is then crystalized within the secretory granules. Insulin is stored in these granules in a hexameric-structure, where two Zn^{2+} ions coordinating six insulin monomers. This storage form is critical for efficient insulin release when blood glucose levels rise, enabling proper glucose regulation throughout the body [24]. In the dithizone staining assay, the dithizone dye (DTZ) is zinc-chelating agent that binds to the Zn^{2+} ions in the insulin secretory granules, selectively staining them a crimson red color [25].

When glucose concentrations of the bloodstream are low (<3mM), the beta-cells are hyperpolarized due to the open of K_{ATP} channels and minimal Ca^{2+} ion influx, resulting in basal insulin secretion. As blood glucose levels rise, the cytosolic ATP/ADP ratio increases, causing the

K_{ATP} channels to close. This depolarization triggers the opening of voltage-gated Ca^{2+} channels, leading to an increase in the influx of Ca^{2+} ion into the cell. The influx of this cation activates an effector system that induces the exocytosis of insulin-secretory granules. Disturbances of this mechanism can result in impaired insulin secretion, contributing to the development of diabetes [22,26].

2.3. Type I diabetes mellitus

When blood glucose levels are inadequately controlled due to disruptions in the insulin secretion mechanism, the heterogeneous metabolic disorder known as diabetes mellitus (DM) develops. DM can be classified into several types, including Type 1 diabetes (T1DM), Type 2 diabetes (T2DM), maturity-onset diabetes of the young (MODY), gestational diabetes, and neonatal diabetes [27,28]. In this study, we focused on T1DM.

T1DM is a chronic autoimmune disease where the immune-mediated destruction of the insulin-producing beta-cells, located in the islets of Langerhans, takes place [29]. It accounts for 5-10% of all diabetes cases [30]. The exact etiology of this immune disorder remains unclear; however, it is hypothesized that environmental triggers play a key role in activating innate and adaptive mechanisms leading to autoreactive T and B cells replication. This immune response ultimately results in the destruction of approximately 80-90% of the beta cell mass [31].

The primary treatment for T1DM is the continuous administration of exogenous insulin. However, maintaining controlled glycemic levels remains a significant challenge. Failure to achieve glycemic homeostasis can lead to severe secondary complications, including kidney failure cardiovascular diseases, blindness, and limb amputation [31,32]. When insulin therapy fails to

provide adequate glucose control, islet transplantation becomes a viable alternative treatment for T1DM [33].

2.3.1. Conventional therapeutics

The discovery of insulin revolutionized the diagnosis and treatment of diabetes. Before its discovery in 1922 by Frederick Banting, John Macleod, and Charles Best at the University of Toronto, diabetes was considered a dead sentence, with a dreadful prognosis and significant reduced quality of life [34].

After its discovery, the administration of exogenous insulin became the primary treatment for T1DM. Patients with T1DM require multiple insulin injections throughout the day. There are several methods of administration, including syringes, insulin pumps, and prefilled pens, each offering different benefits and convenience. In addition to insulin administration, continuous glucose monitoring, carbohydrate counting, and proper training in adjusting insulin doses based on physical activity and carbohydrate intake are essential. These strategies help patients effectively manage their condition and avoid hyperglycemic or hypoglycemic episodes. Long-term complications of hyperglycemia encompass both microvascular and macrovascular issues. Microvascular complications include nephropathy, retinopathy, and neuropathy, while macrovascular complications involve heart failure, cerebrovascular disease, and peripheral artery disease. Additionally, hypoglycemia can impair cognitive function and may be life-threatening [35–37].

Although insulin therapy is sufficient to maintain physiological glucose homeostasis for most patients, some individuals are unable to achieve this with exogenous insulin injections. These patients may experience severe hypoglycemic episodes or hypoglycemic unawareness. For such

patients, human islet transplantation is recommended [38]. The Edmonton Protocol was developed by Shapiro *et al.* at the University of Alberta in 2000. Under this protocol, islets are isolated, purified, and transplanted via the portal vein [39]. It was reported that between 2007 and 2010, islet graft survival, defined by C-peptide levels ≥ 0.3 ng/mL, was 92% during the first year and 83% at the third year, with 44% of patients achieving insulin independence [40].

2.4. SC-islets as an alternative cell source

Islet transplantation is an established and widely recognized therapeutic treatment for patients with severe type I diabetes mellitus (T1DM), particularly when conventional therapies, such as exogenous insulin, are insufficient to maintain proper blood glucose levels [33]. However, the limited availability of donor islets and the necessity for lifelong immunosuppression hinder its broader application [41]. To achieve the required islet concentration (5, 150 – 10, 450 IEQ/kg [42]), typically more than two pancreases are needed. Considering that the islet supply for transplantation is minimal, the differentiation of human pluripotent stem cells (hPSC) into insulin-secreting beta-cells is a promising alternative source for diabetes cellular therapy [2,43].

In 2014, two research groups, Rezania *et al*. and Pagliuca *et al*., published differentiation protocols in which they described the successful generation of pancreatic islet-like clusters from hPSCs [44,45]. Rezania *et al*. described a seven-stage protocol, while Pagliuca *et al.* proposed a six-stage protocol. Both groups reported the generation of approximately 40% NKX6.1-positive insulin-producing beta cells. Although both protocols successfully produced insulin-producing cells derived from hPSCs, when compared to primary human islets, the differentiated cells revealed that they remained immature. Similar results were reported by Hogrebe *et al.* and Balboa *et al.* where, despite the promising functional outcomes of these *in vitro* cells, the transcriptional profile of SC-derived beta cells more closely resembled that of primary human islets after long-

term *in vivo* transplantation [46,47]. Table *1* provides an overview of SC-islet differentiation protocols developed by various research groups.

Table 1. Overview of different SC-beta cell differentiation protocols

Protocol	Number of stages	Format	Quality control outcomes
Rezania *et al*. (2014) [44]	7	Adherent culture until stage 4, followed by a 3D culture system	~45% mono-hormonal pancreatic β-cells at the final stage. Transplanted stage 7 cells successfully reversed diabetes in mice within 40 days.
Pagliuca *et al*. (2014) [45]	6	3D cell culture system	~38% NKX6.1+ insulin-producing β-cells.
Russ *et al*. (2015) [48]	5	3D culture system	~25% NKX2.2+ insulin-producing β-cells.
Velazco-Cruz *et al.* (2019) [2]	6	3D culture system	~52% NKX6.1+ c-peptide-producing β-cells
Hogrebe *et al.* (2020) [46]	7	3D cell culture system	Transplanted SC-β cells effectively reversed diabetes in mice, maintaining normoglycemia for up to 9 months.
Balboa *et al.* (2022) [47]	7	Adherent culture until stage 4, followed by a 3D culture system	After transplantation, SC-β cells exhibited further *in vivo* maturation, upregulating key β-cell markers such as MAFA, G6PC2, and UCN3.
Braam et al. (2023) [49]	7	Adherent culture until stage 4, followed by a 3D culture system	~60% NKX6.1+ insulin-producing β-cells.

2.4.1. Scale-up production

Conventional 2D cultures present scale-up limitations due to the large surface area required to culture significant amounts of cells. Additionally, these cultures demand a high number of culture dishes and considerable user handling, which increases the risk of contamination. Furthermore, batch variability, along with the lack of process standardization and control, presents major limitations for clinical applications [6]. To address these challenges, 3D stem cell culture has

been developed. The culture of hPSCs in stirred tank bioreactors has been widely adopted for large-scale production [50,51].

Several stem cell-derived islet differentiation protocols have been developed using hPSC aggregates [52–54]. This 3D environment has the potential to enhance process scale-up, facilitating the translation of bench technologies into clinical-scale manufacturing and supporting further commercialization. However, one key challenge is controlling aggregate size. Large aggregates can face limitations in mass transfer, leading to the formation of a necrotic core and cell loss. Additionally, the heterogeneity in size distribution may create variations in morphogen levels between aggregates, due to differences in the diffusion of growth factors and small molecules [55–57].

2.5. Encapsulation techniques and their applications on cell culture and transplantation

The use of artificial immunoprotected microenvironment to prevent rejection of transplanted human islets or SC-islets have been studied. Semi-permeable biomaterials have been used to encapsulated islets. This encapsulation creates a microenvironment that allows the diffusion of oxygen, glucose, nutrients, and hormones like glucagon and insulin, while preventing the graft cells from migrating to other parts of the body and blocking the entry of immune cells. These characteristics may improve graft survival and reduce the need for immunosuppressants [33,58]. Furthermore, encapsulation facilitate handling and retrieval of the cell product [59]. These encapsulation devices are mainly made out of polymers like polytetrafluoroethylene (PTFE) or alginate hydrogels; however, these devices could be prone to fibrosis, which can limit nutrient diffusion [59].

2.5.1. Encapsulation in microbeads for biomanufacturing

The use of 3D structures during the hPSC differentiation process more closely resembles the *in vivo* physiological environment. Additionally, it enables the scalable expansion of these cells. Although high-fold expansion can be achieved in suspension culture, there are inherent limitations, such as difficulty in producing uniformly sized spheroids and challenges in enhancing nutrient transport through agitation while preventing cell loss due to hydrodynamic shear stress. To address these issues, encapsulating hPSCs in microbeads – also termed microencapsulation - has been employed to protect the cells from shear-induced damage caused by the impeller of the mixing system [6,7].

Fattahi *et al*. [7] proposed a poly(ethylene glycol) hydrogel microfluidic-based encapsulation system for hPSCs, with an aqueous core to promote spheroid formation and facilitate further pancreatic beta-cell differentiation. They reported the successful formation of spheroids resulting from the encapsulation of single hPSCs. The capsule did not affect the pluripotency of the clusters, which they demonstrated by differentiating them into pancreatic beta-cells, yielding 17% insulin-producing cells. They highlighted that the hydrogel microcapsule provided protection from shear stress, withstanding forces of up to 3 Pa.

2.5.2. Microencapsulation methods

Conventional encapsulation methods include coaxial air-flow, vibration, and electrostatic techniques, all of which rely on the formation of individual droplets using a nozzle tip, followed by solidification through physical or chemical mechanisms [60]. The coaxial air-flow method involves a cylindrical reservoir containing the hydrogel-cell mixture to be encapsulated. The droplets are propelled through a nozzle by a constant and controlled stream of compressed air, depositing into a cross-linking solution [61]. The electrostatic method can be used to control droplet

size. It involves the formation of droplets by applying an electrostatic voltage. This physical force is applied to the metal nozzle, inducing an electric charge in the liquid passing through the nozzle. The droplets formed under the influence of electrostatic forces are smaller than those formed without them [62].

Nozzle-based encapsulation methods present significant challenges for scaling up due to their low throughput, typically ranging from approximately 10 to 360 mL/h. Additionally, these methods are limited to low-viscosity fluids and the size of the clusters being encapsulated, as they depend on the nozzle size. Nozzle-based encapsulation techniques also generate high shear forces at the nozzle tip, which can reduce cell viability. Furthermore, using high-viscosity fluids can lead to clogging of the nozzle tip. As a result, nozzle-based encapsulation is inefficient and unsuitable for encapsulating SC-islets or human islets, particularly when working with high-viscosity materials [60,63–65].

2.5.3. Emulsion-based microencapsulation

Hoesli *et al.* first described the immobilization of mammalian cells using an emulsion-based encapsulation method. This method was adapted from a previously developed protocol (Poncelet *et al*. [66]). It involves the alginate internal gelation, in contrast to the conventional nozzle-based encapsulation method, which uses external gelation (where alginate droplets are extruded into a calcium salt solution [67]).

The emulsion-based microencapsulation process (internal gelation) consisted of two phases: the organic phase containing mineral oil, and the aqueous phase, which included alginate, cells, and $CaCO_3$ (non-soluble form of calcium). The cell mixture goes through an emulsification step. Following emulsification, the environment is acidified by adding an oil-soluble acid (e.g.

glacial acetic acid) for an acidification step. The resulting drop in pH leads to the internal release of Ca^{2+} and the gelation of the alginate droplets into beads [68]. The slow gelation involved in this mechanism allows for the formation of more homogeneous gel networks compared to the external gelation method [69].

The method outlined above is the one employed in this study. To our knowledge, no SC-islets have been immobilized in alginate beads generated by emulsion-based encapsulation and interna gelation using stirred vessels.

2.5.4. Preclinical and clinical testing of encapsulated SC-islets and human islets

2.5.4.1. Microencapsulation

Microencapsulation involves embedding cells within microscale capsules [70]. Several research groups have demonstrated the potential of this technique for diabetes treatment. The semi-permeable membrane of the capsules could potentially eliminate the need for immunosuppressive drugs by serving as a physical barrier between the host immune system and the transplanted cells, while still allowing the diffusion of essential nutrients and hormones such as insulin [70,71]. Bochenek *et al.* [72] transplanted microencapsulated allogeneic pancreatic islets into the omental bursa of macaques. Their modified alginate capsules successfully prevented pericapsular fibrotic overgrowth, and the explanted islets retained 90% viability after four months without the use of immunosuppression.

The Calafiore group at the University of Perugia developed an alginate ultrapurification process to obtain clinical-grade alginate for microcapsule fabrication. This advancement enabled them to conduct numerous preclinical studies in which both allogeneic and xenogeneic encapsulated islets were transplanted into non-immunosuppressed animal models. Following three

decades of research evaluating the safety and efficacy of their system, they launched a pilot Phase I clinical trial [71]. In this study, four non-immunosuppressed patients with T1D received transplants of microencapsulated human islets. The results demonstrated that none of the patients experienced adverse reactions to the grafts, and C-peptide levels were detectable for periods ranging from 100 to 480 days. Moreover, no islet-specific antibodies—such as anti-MHC class I/II or anti-GAD65—were detected. These findings indicated that the microcapsules effectively protected the transplanted islets from the host immune system, even in the absence of immunosuppressive therapy [73].

Other groups have evaluated the functionality of alginate-microencapsulated human islet grafts compared to non-encapsulated cells. Tulleneers-Thevissen *et al.* [74] assessed this in immunodeficient non-obese diabetic (NOD) mice. Their findings showed that free (non-encapsulated) islet grafts began lowering blood glucose levels by day 1 post-transplant, indicating initial functionality. However, by the end of the first week, all recipients experienced episodes of hyperglycaemia. In contrast, mice receiving microencapsulated human islets achieved normoglycaemia by week 1 and maintained stable glucose levels through the end of the study at week 30.

2.5.4.2. Macroencapsulation

Several companies have developed macroencapsulated transplantation devices containing SC-islets, leading to clinical trials. The company ViaCyte developed the PEC-Encap macroencapsulation device, which contains SC-pancreatic progenitors. In 2014, they launched a Phase I/II clinical trial to evaluate the implantation of this device in patients with type 1 diabetes. The device was designed to be cell-impermeable, making it immunoprotective. However, two years after implantation, insulin-immunoreactive cells were observed in some explanted devices,

and insulin secretion was not detected [75]. In 2017, ViaCyte initiated another clinical trial with a modified version of the macroencapsulation device, named PEC-Direct, which was not immunoprotective. As a result, patients required immunosuppression to minimize the risk of both alloimmune and autoimmune responses. After one year of follow-up, data showed that SC-pancreatic progenitors successfully matured *in vivo* into insulin-producing beta cells in patients with T1D. This led to patients achieving meal-responsive C-peptide production following device transplantation [76].

Vertex Pharmaceuticals Incorporated developed two cell therapies for the treatment of type 1 diabetes (T1D): VX-880 and VX-264. VX-880 (NCT04786262) involved the infusion of SC-islets into the portal vein of patients with T1D. In January 2024, Vertex announced a pause in the study due to unrelated patient deaths [77]. However, the trial was recently resumed, and it is now in Phase III [78]. VX-264 is an immunoprotective device containing encapsulated, fully differentiated SC-islets. A Phase I/II study demonstrated that the device was safe and well tolerated by patients. However, C-peptide levels did not reach the threshold necessary for clinical benefit. As a result, in March 2025, Vertex announced that VX-264 would not proceed to further clinical trials [79].

Other companies, such as Beta-O2 Technologies, have also developed macroencapsulation devices for the treatment of type 1 diabetes (T1D). Beta-O2's device, the *βAir Bio-Artificial Pancreas*, contains encapsulated islets and is designed to maximize oxygen flow to enhance cell survival. The device features two ports, requiring the patient to inject oxygen once daily. It is intended for subcutaneous implantation in the lower abdominal area [80].

In their Phase I clinical trial, four non-immunosuppressed T1D patients received transplants of 1,800–4,600 IEQ/kg and were monitored for 3 to 6 months. None of the subjects developed human leukocyte antigen antibodies or showed immune cell infiltration at the device site, demonstrating

the *βAir* system's safety in preventing allogeneic islet rejection and allowing the transplanted cells to remain viable for several months. However, by 3 to 6 months post-transplantation, a thin fibrotic capsule was observed surrounding the device. Additionally, the low levels of circulating C-peptide detected had no significant impact on metabolic control [81]. The clinical trial (NCT02064309) is ongoing, with an estimated completion date in May 2025.

2.5.5. Effect of the encapsulation microenvironment on the stem cell differentiation

External signaling, including chemical and physical cues from the microenvironment, plays a crucial role in driving the differentiation of hPSCs to a specific cell type. These signals are sensed and translated by the integrins. 3D culture systems, which mimic the physiological environment by simulating matrix interactions and physical cues such as microenvironment stiffness, directly influence cellular responses and differentiation [82,83].

Alginate is a linear copolymer composed of (1 → 4)-linked β-D-mannuronate (M) and α-L-guluronate (G) residues. It undergoes gelation in the presence of divalent cations, such as Ca^{2+}, Ba^{2+}, and Mn^{2+}. When these divalent cations are present, two antiparallel G chains are crosslinked by the ions, forming a junction structure known as the "egg-box" configuration [84]. Wilson *et al*. reported that the alginate composition of microcapsules had a direct impact on the expansion and differentiation capacity of ESCs. Encapsulation in high α-l-guluronic acid (G) alginates (stiffer microenvironment) resulted in slower cell proliferation and a loss of pluripotency compared to more viscoelastic beads with high β-d-mannuronic acid (M) content or non-encapsulated clusters [85].

Interestingly, Oda *et al.* found that the proliferation of mesenchymal cells was closely related to the storage modulus (G') of the hydrogel. When cells were encapsulated in hydrogels

with a high G' value (stiffer material), cell proliferation was halted, and the cells entered the G1 phase. In contrast, when cells were encapsulated in hydrogels with G' values below 1.0 kPa, cell proliferation was not significantly affected [86].

Similar results were reported by Richardson *et al.* [87] who reported that low-stiffness barium alginate capsules with a Young's modulus ranging from 4 to 7 kPa supported hESC growth and viability. In contrast, stiffer capsules suppressed cell growth. However, when examining the effect of microenvironment stiffness on pancreatic differentiation, the impact varied depending on the differentiation stage. An increase in stiffness promoted definitive endoderm differentiation due to the upregulation of TGF-beta signaling. In contrast, stiffer environments at later stages suppressed pancreatic progenitor differentiation due to the upregulation of Sonic Hedgehog signaling.

3. Thesis Objectives

The goal of this project was to investigate whether alginate microencapsulation can protect SC-islets from agglomeration and local energy dissipation, while also studying the effect of the alginate microenvironment on the maturation of SC-islets. We hypothesized that alginate immobilization would enable scale-up by creating a local environment that would prevent agglomeration, exposure to high shear, and potentially also afford control over differentiation mechanisms.

(1) Study the effect of the seeding density when aggregating pancreatic endocrine precursors cells on the SC-islets differentiation.
(2) Analyze the effect of different alginate concentrations during the encapsulation process on the differentiation of SC-islets.
(3) Test whether the encapsulation method enables the scale-up process by protecting the SC-islets from the mechanical stress caused by the impeller.

4. Materials and Methods

4.1. Cell source and maintenance

Human ESCs (WA01 H1, WiCell) were used under Stem Cell Oversight Committee approval, and used at passage 25-30. Following thawing, the cells were cultured on Sarstedt (red) plates previously coated for 120 min with hESC-qualified Matrigel, Corning™, 354277, using 0.21 mL/cm^2 mTeSR™1 medium (STEMCELL Technologies, 85850). Upon reaching 70-80% confluency, they underwent clump passaging, cells were washed with Ca^{2+} and Mg^{2+} free DPBS (Gibco™, 14190144), incubated for 4 min with 0.5 mM UltraPure™ Ethylenediaminetetraacetic acid (EDTA) (in Ca^{2+} and Mg^{2+} free Dulbecco's phosphate-buffered saline (DPBS)), pH 8.0, Invitrogen™, 15575020. Following incubation, the EDTA solution was discarded and replaced with mTeSR™1 media. The clumps were detached from the surface using a cell scraper (Sarstedt, 83.3950), and gently disaggregated into smaller clumps using a 10 mL pipette, then reseeded at a 1:10 dilution.

After passaging, the cells were reseeded on fresh Matrigel-coated plates. Daily media changes were performed with mTeSR™1 medium, typically ± 3 h from the initial seeding time. After three to four rounds of clump passaging, pancreatic differentiation was initiated. Human islets were obtained from the Alberta Diabetes Institute Islet Core.

4.2. Stem cell-derived pancreatic islet differentiation

The pancreatic differentiation protocol was carried out as previously described [44,47,53,88], with minor modifications. The H1 used for this process had a passage number between 30 and 40. Culture surfaces were pre-coated with growth factor-reduced Matrigel (Corning™, 35623) for 120 min. A seeding density of 130,000 cells/cm^2 and 0.21 mL/cm^2 mTeSR™1 medium was used.

Media changes were performed daily from stage 1 to stage 6, and every other day during stage 7, typically ±1 h from the previous feeding time. At stage 4, day 4, aggregates were formed using the AggreWell™ 400 6-well plate (STEMCELL™ Technologies, 34425). Cells were harvested from the culture plate surface using TrypLE™ Select Enzyme (1X) (Thermo Fisher Scientific, 12605010). Three seeding densities were evaluated: 500, 1000, and 1500 cells per microwell. Based on the study, the seeding density moving forward was 1000cells/microwell. At stage 5, day 7, the aggregates were transferred to ultralow attachment plates (Corning, CLS3471-24EA) and placed on a CellTron CO_2 resistant shaker (Infors, 510925) orbital shaker set to an agitation rate of 100 rpm. Aggregates were encapsulated on day 7 of stage 6, followed by another transfer to ultralow attachment plates and placement on a Celltron orbital shaker at 100 rpm (for Objectives 1 and 2) or in a 100 mL PBS mini bioreactor at an agitation rate of 60 rpm [53]. The bioreactors were seeded at a cell concentration of $1.5x10^5$ cells/mL. Every 48 h media changes were performed with stage 7 complete medium, typically ± 3 h from the initial seeding time. Figure 2 shows the schematic representation of the pancreatic differentiation protocol. The media formulation, growth factors, and small molecules used are detailed in Table 2.

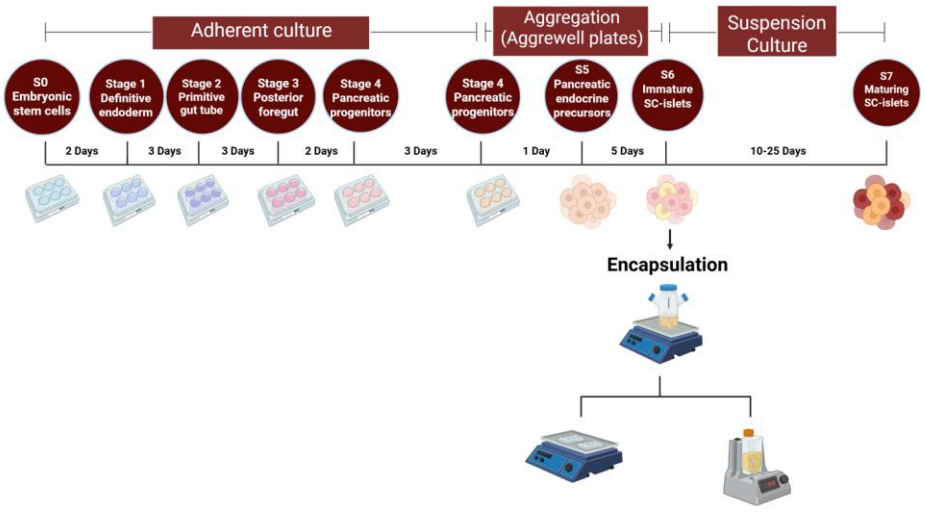

Figure 2. Schematic representation of the pancreatic differentiation protocol workflow. Created with BioRender.com

4.3. Hydrogel preparation

A 50:50 mixture of the ultrapure sodium alginate PRONOVA^{TM} UP MVG (Novamatrix, Catolog #4200101) and PRONOVA^{TM} UP LVM (Novamatrix, Catolog # 42000001) was used to prepare 2.43%, 6.0% and 8.5% alginate stock solutions to respectively obtain 2%, 5% and 7% alginate beads (notwithstanding swelling). The alginate powder was dissolved in HEPES buffer consisting of 10 mM 4-(2-Hydroxyethyl) piperazine-1-ethanesulfonic acid, N-(2-Hydroxyethyl) piperazine-N′-(2-ethanesulfonic acid (HEPES; Thermo Fisher Scientific, BP310-500), and 170 mM NaCl (Sigma Aldrich, S9888) at pH 7.4, and then autoclaved at 121°C in a humid vapor cycle for 30 min (STERIS, AMSCO® Lab 110-250).

4.4. Emulsion-based encapsulation and internal gelation

The emulsion-based encapsulation and internal gelation method previously described[64,68] was followed with some modifications. Immature SC-islets (stage 6 day 7) were used in the encapsulation process.

An aqueous cell mixture was prepared as follows: 1.24 mL of alginate stock solutions, 130 µL of 0.5 M $CaCO_3$ solution in 10 mM HEPES buffer (Skyspring Nanomaterials, 1951RH), and 137 uL of SC-islets solution ($2.0x10^4$ cells/µL). The mixture was gently homogenized using a stainless-steel laboratory spatula.

Fist, 40 mL of light mineral oil (Thermo Fisher Scientific, O121-1) was agitated at 300 rpm for 2 min in a 100 mL microcarrier spinner flask (Bellco, 1965-00100) with modified perforated impeller (Figure 3C). After this initial agitation, the stirring speed was reduced to 210 rpm. The aqueous cell mixture was then added dropwise to the spinner flask and emulsified for 12 min. The agitation rate between conditions was adjusted to ensure a consistent volume mean

diameter (D_{43}) for the beads across all conditions. The stirring speeds for the 2%, 5%, and 7% alginate beads were 240, 380, and 460 rpm, respectively.

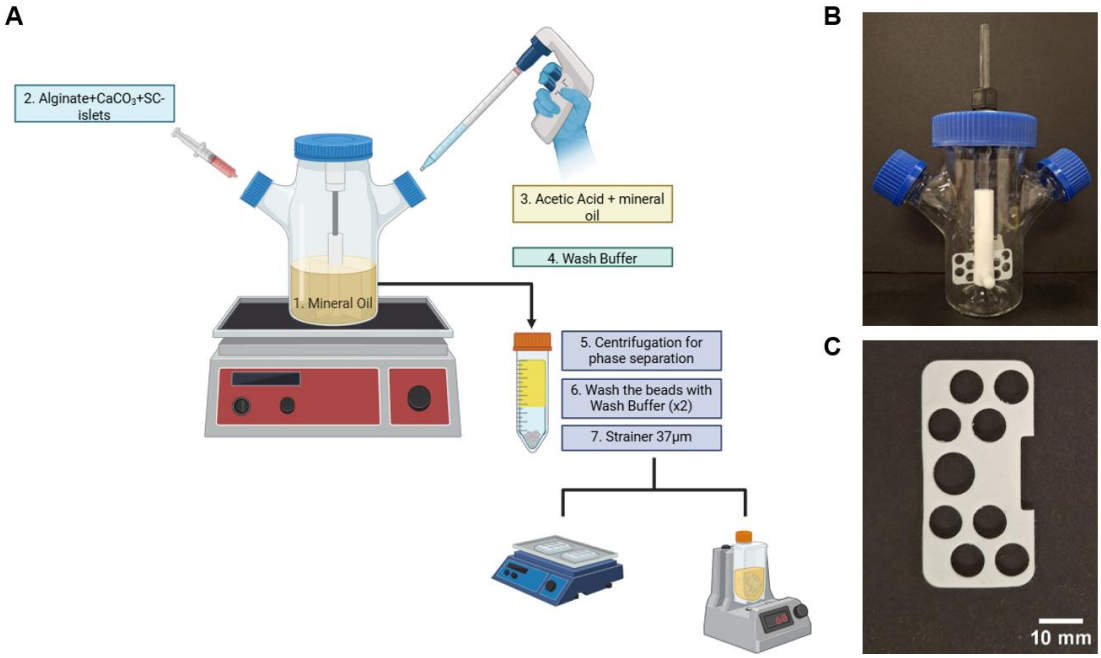

Figure 3. Emulsion-based encapsulation device and the microbead production process. **(A)** Schematic drawing of the SC-islets emulsion-based encapsulation process. Created with BioRender.com **(B)** Photograph of the emulsion-based encapsulation device (Micro-carrier Spinner Flask, BELLCO, 1965-00100). **(C)** Photograph of the impeller used in the emulsion-based encapsulation process.

Following the emulsification, 10mL of acidify light mineral oil (9.64 µL glacial acetic acid dissolved through vertexing in 10mL light mineral oil immediately prior to starting the process) was added to the spinner flask for an 8 min acidification step. Subsequently, 40mL of wash buffer (11.025 g/L $CaCl_2$, 4.38 g/L NaCl, and 2.383 g/L HEPES, pH 7.4) mixed with 10% stage 7 media was added to neutralize the pH. The oil, beads, and aqueous solution from the spinner flask were retrieved and collected in 50mL Falcon tubes for centrifugation at 300 × g for 5 min. The oil was removed by aspiration, taking care to remove oil at the interface. Two more washes were performed. The beads were strained using a 37 µm reversible strainer (Stem Cell Technologies,

27250). The encapsulated SC-islets were further transferred to ultralow adhesion 6-well plates or 100 mL PBS mini bioreactor. Figure 3A shows a schematic representation of the SC-islets emulsion-based encapsulation process.

4.5. Cell quantification

A degelling solution was prepared using 8.8 g/L sodium citrate tribasic dihydrate (Sigma Aldrich, C8532), 2.63 g sodium chloride (Sigma Aldrich, S5886), 1.19 g/L HEPES (Thermo Fisher Scientific, BP310-500), and adjusted to pH 7.4. This solution was used to recover immobilized SC-islets. Harvested clusters were washed twice with DPBS (without Ca^{2+} or Mg^{2+}) and then dissociated into single cells using TrypLe. The aggregates were incubated at 37°C for 8-10 min. After dissociation, single cells were resuspended in fresh media for subsequent cell counting. Both manual counting (using a Bright-Line™ Hemacytometer, Sigma Aldrich) and automatic counting (using a TC20 Automated Cell Counter, Bio-Rad) were performed to quantify cell concentration.

4.6. Flow cytometry

The method previously described by Brassard *et al.* [89] was followed. Cell monolayers or clusters were harvested and washed twice with DPBS (without Ca^{2+} or Mg^{2}), then dissociated into single cells using TrypLe. Clusters were incubated at 37°C for 8-10 min. After dissociation, single cells were resuspended in FACS Buffer (DPBS supplemented with 2% FBS [89]). Next, the cells were incubated in the dark for 30 min with fixable viability dye (Life Technologies, L34963), washed twice with FACS Buffer, and fixed and permeabilized using Cytofix/Cytoperm (BD Biosciences, 554714) for 10 min.

The conjugated antibodies used are detailed in Table 5. Fixed cells were incubated with the conjugated antibodies for 30min in the dark, washed twice with Perm/Wash buffer (BD

Biosciences, 554723), and then resuspended in FACS buffer for analysis. Flow cytometry was performed using BD Accuri™ C6 Plus Flow Cytometer, and the data were analyzed using FlowJo™ v10 software.

4.7. Dithizone staining

The protocol previously described by reference [53] was followed. Dithizone powder (Sigma-Aldrich, 43820) was reconstituted in Dimethyl sulfoxide (DMSO) (Fisher Scientific, BP231-100) and subsequently diluted in DPBS (without Ca^{2+} or Mg^{2}) to a final concentration of 0.5mg/mL. The solution was filtered using 0.2 µm syringe filters (Fisher Scientific, 13100106) to eliminate any particulate matter. The aggregates were stained in the Dithizone solution for 1-2 min, followed by multiple rinses (~10) with Ca^{2+} and Mg^{2+} free DPBS. Images were captured using a Zeiss Stemi 2000-C Stereo Microscope (455053) and Samsung Galaxy A32 smartphone.

4.8. Live/Dead staining

Encapsulated and non-encapsulated SC-islets were incubated for 20min at 37ºC using a live/dead staining solution containing18.9 µg/mL Propidium Iodide (Fisher Scientific, P1304MP) and 1.1 µg/mL Calcein AM (Fisher Scientific, C3099). The clusters were then visualized, and images were acquired using IX81 Olympus Microscope with the FITC filter cube (Ex: 482/35 | Em: 536/40) and the Texas Red filter cube (Ex: 525/40 | Em: 585/40) [89]. ImageJ software was utilized for image processing.

4.9. Static glucose-stimulated insulin secretion (GSIS)

The protocol previously described by Brassard *et al.* [89] was followed with minor modification. To assess the SC-islets' ability to secrete insulin in response to varying glucose concentrations, 20 encapsulated and non-encapsulated SC-islets, as well as human islets, were

hand-picked. The clusters were first incubated for 1 h in Krebs buffer supplemented with 2.8 mM glucose to equilibrate the system to basal glucose levels [56]. The basal Krebs buffer (no glucose) was prepared as follows: 129 mM NaCl (Sigma Aldrich, S9888), 4.7mM KCl (Sigma Aldrich, P3911), 2.5mM $CaCl_2 \cdot 2H_2O$ (Sigma Aldrich, Catalog # 223506), 1.2mM $MgSO_4$ (Sigma Aldrich, 7487-88-9), 1.2mM KH_2PO_4 (Sigma Aldrich, 7778-77-0), 5.0mM $NaHCO_3$ (Thermo Fisher Scientific, 144-55-8), 10mM HEPES (Thermo Fisher Scientific, Catalog # BP310-500), 0.1% BSA (Sigma Aldrich, A3294), pH 7.4.

Subsequently, the clusters underwent a series of incubations: first in Krebs buffer supplemented with 2.8 mM glucose (low glucose incubation, 1 h), followed by Krebs buffer supplemented with 16 mM glucose (high glucose incubation, 1 h), then Krebs buffer with 2.8 mM glucose again (second low glucose incubation, 1 h), and finally Krebs buffer supplemented with 30 mM KCl (1 h). Two washes with Krebs buffer supplemented with 2.8 mM glucose were performed between the high glucose and second low glucose incubations. All samples were stored at -20°C until analysis.

Insulin secretion was measured using the Human C-Peptide ELISA Kit (ALPCO, 80-CPTHU-E01.1) following the manufacturer's instructions. Absorbance (450 nm) of all samples was measured using the Benchmark Plus Microplate Spectrophotometer (Bio-Rad).

4.10. Mechanical properties of the beads

To analyze the mechanical properties and viscoelasticity of different alginate bead formulations (2%, 5%, and 7%), the protocol described by Shin *et al.* [90] as followed. The MicroSquisher (CellScale), equipped with a parallel-plate compression configuration and a 559 μm diameter microbeam, was used for testing. Beads with the following size ranges were

evaluated: 1100–1700 µm (2% alginate), 950–1100 µm (5% alginate), and 875–1200 µm (7% alginate). The beads were placed on a metal platform inside a chamber filled with Wash Buffer solution (see Section 4.4) at room temperature. To measure force as a function of displacement, the SquisherJoy software was utilized. Each bead underwent three consecutive cycles of up to 30% volume compression, with the following time settings: 30 seconds of loading, 10 seconds of holding, and 30 seconds of recovery. The Young's modulus (or compressive modulus, E) for each bead at 10%, 20%, and 30% compressive volume was calculated using MATLAB software and the Hertzian half-space contact model (refer to Equations 1, 2, 3, and 4) [90,91].

$$E = \frac{3(1-v^2)F}{4\delta a} - \frac{f(a)F}{\pi\delta} \quad (1)$$

$$f(a) = \frac{2\,(1+v)R^2}{(a^2+4R^2)^{\frac{3}{2}}} + \frac{1-\,v^2}{(a^2+4R^2)^{\frac{1}{2}}} \quad (2)$$

$$a = (R-\,\delta)\tan\theta \quad (3)$$

$$\theta = \,cos^{-1}\left(\frac{R-\,\delta}{R}\right) \quad (4)$$

4.11. Aggregate size measurement

To assess the aggregate size at various stages, brightfield images were captured using a VWR® Trinocular Inverted Microscope. Image analysis of the aggregates' size was conducted using ImageJ software. Equations 5, 6, and 7 were used to determine the estimated radio (r), diameter (d) and volume (V) of the aggregates:

$$Radio\ (r) = \sqrt{Area \cdot \pi} \quad (5)$$

$$Diameter\ (d) = 2 \cdot r \tag{6}$$

$$Volume\ (V) = \frac{4 \cdot \pi \cdot r^3}{3} \tag{7}$$

4.12. Statistical analysis

The statistical analysis was performed using the GraphPad Prism software. Data normality was assessed using the Shapiro-Wilk test, and P-values < 0.05 were considered statistically significant. For parametric data, one-way ANOVA with Tukey's multiple comparisons test was used. Non-parametric data were analyzed using Brown-Forsythe ANOVA test with Games-Howell's multiple comparisons test, or the Kruskal-Wallis with Dunn's multiple comparison test. Graphs were generated using GraphPad Prism and Microsoft Excel. Data are presented as the mean ± standard deviation of independent experimental replicates.

5. Results

5.1. Effect of aggregate size on stem cell-derived islet differentiation

To investigate the impact of aggregate size on pancreatic differentiation, pancreatic progenitor cells (stage 4) were aggregated using the AggreWell™ 400 6-well Plate (STEMCELL™ Technologies) at three different seeding densities: 500, 1000, and 1500 cells per microwell. Figure 4A illustrates the changes in aggregate size across different conditions at stage 5, 6, and 7. These changes in size were likely due to the agglomeration of aggregates. Figure 4B presents the percentage of total cell recovery, normalized to the seeding density, during aggregate formation at stage 4 (Pancreatic endoderm). The data reveal significant cell loss during the endocrine differentiation process. On Day 10 of stage 7, the average total cell recovery across all conditions was below 20%, with no significant differences in cell loss between the conditions. Figure 4C shows the size distribution for each condition at each stage, where cluster fusion was notably prominent between stage 5 and stage 6.

Additionally, the analysis of pancreatic marker expression at stage 7, Day 10 (S7D10) of maturation (Figure 5) revealed no significant differences between conditions. NKX6.1 and NEUROD1 expression remained consistently high across all conditions, while the expression of Glucagon and C-peptide was approximately 20% in each condition.

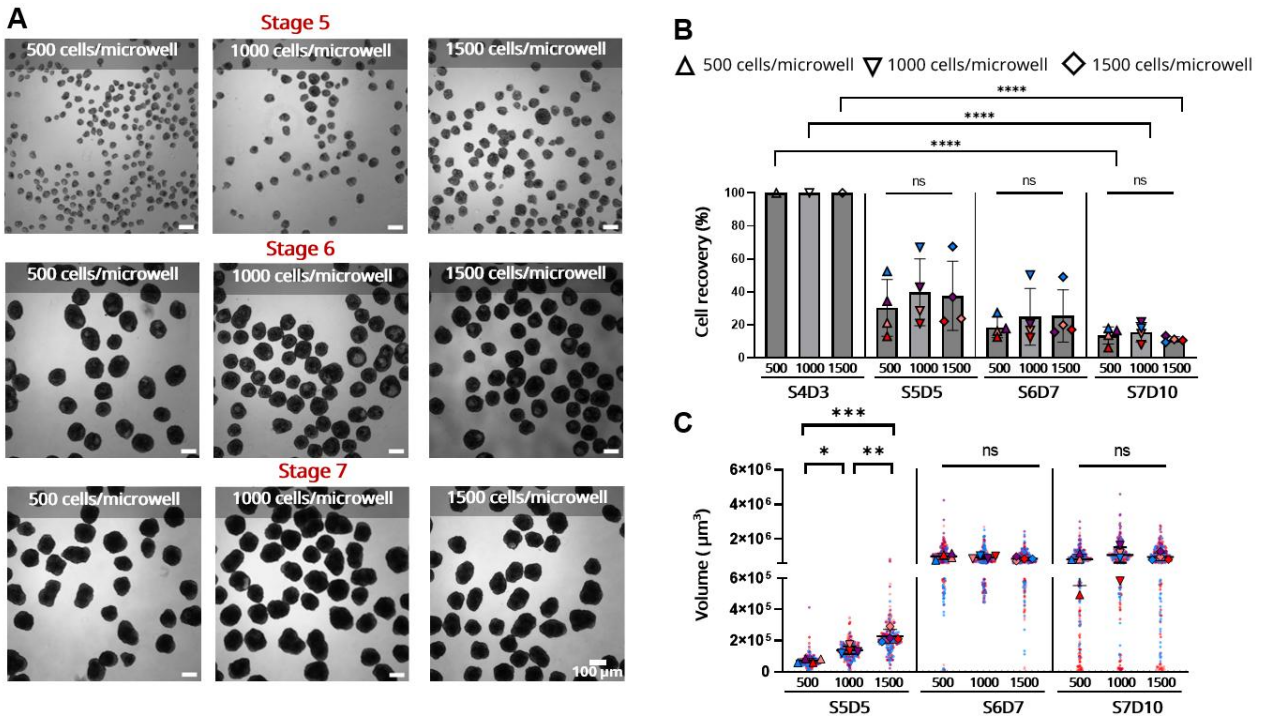

Figure 4. Changes in aggregate size and total cell recovery across different seeding densities during aggregate formation (500, 1000, and 1500 cells/microwell) at various developmental stages. **(A)** Morphological images and aggregate sizes at stage 5, 6, and 7 for each condition. **(B)** Percentage of total cell recovery normalized by seeding density during aggregate formation (stage 4) at each stage (N=4). Statistical significance was determined by two-way ANOVA with Tukey's multiple comparisons test. **(C)** Graph showing size distribution across stages for each condition. Data are presented as the mean and standard deviation (N=4, n=60). Statistical significance was determined by one-way ANOVA with Tukey's multiple comparisons test (Stages 5 and 6) and Kruskal-Wallis with Dunn's multiple comparison test (stage 7). *$p < 0.05$, **$p < 0.01$, ***$p < 0.001$, ****$p < 0.001$. S4D3 = stage 4 day 3, S5D5 = stage 5 day 5, S6D7 = stage 6 day 7, S7D10 = stage 7 day 10

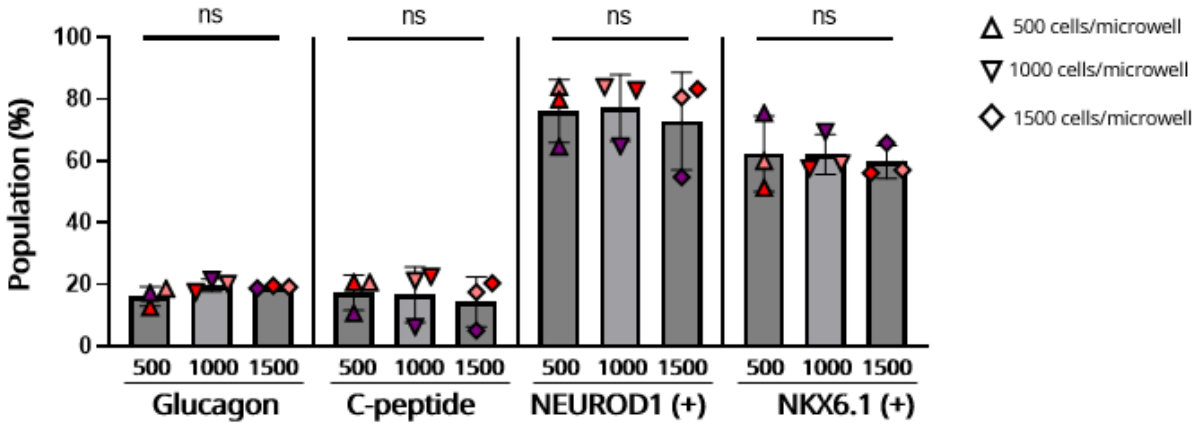

Figure 5. Flow cytometry analysis of pancreatic marker expression at stage 7 (day 10) of maturation. Statistical not significance was determined by one-way ANOVA with Tukey's multiple comparisons test

5.2. Effect of alginate stiffness on pancreatic differentiation

To study the effect of alginate concentration on SC-islet differentiation, we analyzed the mechanical properties of different capsules and assessed the composition and functionality of the clusters after 25 days of immobilized culture.

5.2.1. Mechanical properties of 2%, 5%, and 7% beads

Figure 6A illustrates the volume moment mean diameter (D_{43}) of 2%, 5%, and 7% beads. During the emulsion-based encapsulation process, the agitation rate was adjusted to achieve beads with similar D_{43}. Important to note that D_{43} is representative of the bead diameter in which the average cell would be located. The graph indicates that no significant differences in the volume moment mean diameter were observed across the different conditions.

Three different alginate concentrations (2%, 5%, and 7%) were tested to evaluate whether the stiffness of the capsule microenvironment influenced pancreatic differentiation, particularly during the maturation stage. The Hertzian half-space contact model was applied to calculate the

compressive modulus, or Young's modulus (E), for each condition at 10%, 20%, and 30% volume compression (Figure 6B).

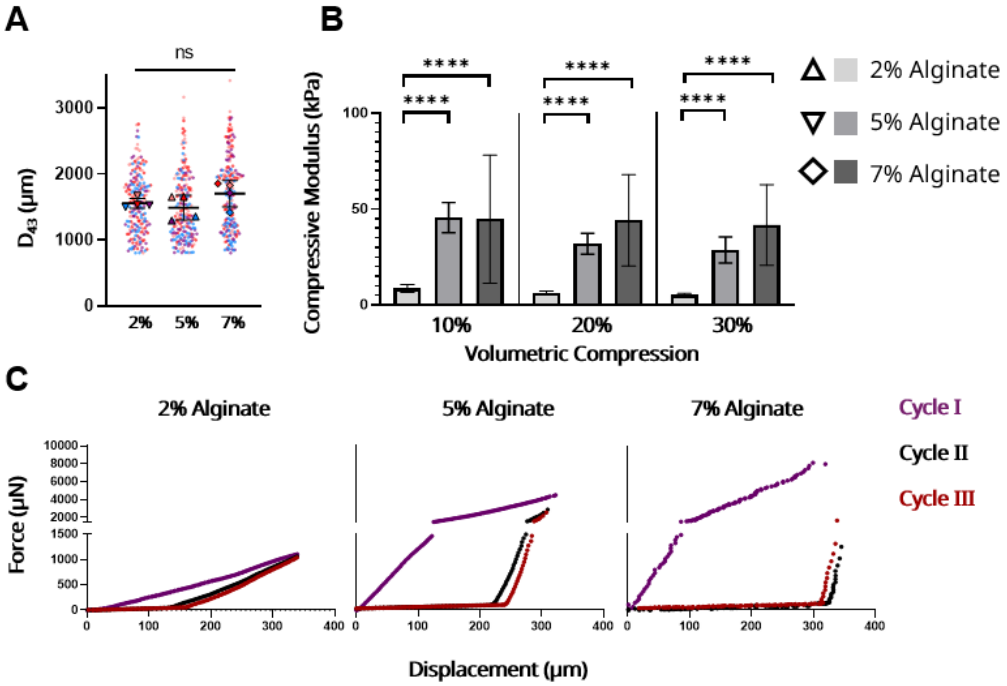

Figure 6. Bead size and mechanical properties of alginate beads formed through emulsion-based encapsulation within 24 hours after production. **(A)** Volume moment mean diameter (D_{43}) of the beads produced with 2, 5, and 7% alginate concentration. Statistical not significance was determined by one-way ANOVA with Tukey's multiple comparisons test (N=4, n=50). **(B)** Compressive modulus of beads at 10%, 20%, and 30% compressive volume for different alginate concentrations (N=3, n=15). Statistical significance was determined by one-way ANOVA with Tukey's multiple comparisons test (10% and 20% compressive volume) and Brown-Forsythe ANOVA test and Games-Howell's multiple comparisons test (30% compressive volume). ****$p < 0.001$. **(C)** Representative viscoelastic behavior of the beads as a function of displacement (µm) vs force (µN). The beads underwent three cycles of up to 30% compressive volume.

As expected, the data showed that higher E values were associated with higher alginate concentrations. Interestingly, no significant differences were observed between the compressive

moduli of the 5% and 7% capsules. Additionally, Figure 6C illustrates the volume displacement of the beads in relation to the applied force across three cycles. All conditions exhibited highly plastic behavior, with the beads permanently deformed and unable to return to their original shape.

Analyzing the previously presented data, seeding densities of 500, 1000, and 1500 cells per microwell for pancreatic progenitor cluster formation using AggreWell™ 400 6-well plate showed no significant impact on SC-islet maturation, cell recovery percentage, or final aggregate volume (μm^3) across conditions. Therefore, a seeding density of 1000 cells per microwell was selected for subsequent experiments.

5.3. Encapsulation as a strategy to minimize cluster aggregation and reduce cell loss

Analyzing the previously presented data, seeding densities of 500, 1000, and 1500 cells per microwell for pancreatic progenitor cluster formation using AggreWell™ 400 6-well plate showed no significant impact on SC-islet maturation, cell recovery percentage, or final aggregate volume (μm^3) across conditions. Therefore, a seeding density of 1000 cells per microwell was selected for subsequent experiments.

5.3.1. Cluster size and viability

To assess whether SC-islets would withstand the emulsification and internal gelation process, we studied SC-islet viability immediately post-encapsulation, as well as after 25 days of immobilized culture. Notably, at 7% alginate, the agitation speed required to achieve a similar D_{43} between conditions reached relatively high values (480 rpm). These factors could potentially affect the viability of the immature SC-islets (stage 6 day 7). To evaluate this, a live/dead staining was performed 24 h and 25 days after encapsulation (Figure 7). Upon analyzing the images, it was

observed that the viability of the clusters remained high even after 25 days of immobilized culture. However, the SC-islets encapsulated at 7% alginate appeared smaller, likely due to the high mixing speed used during encapsulation, which caused partial disaggregation of the clusters due to mechanical stress.

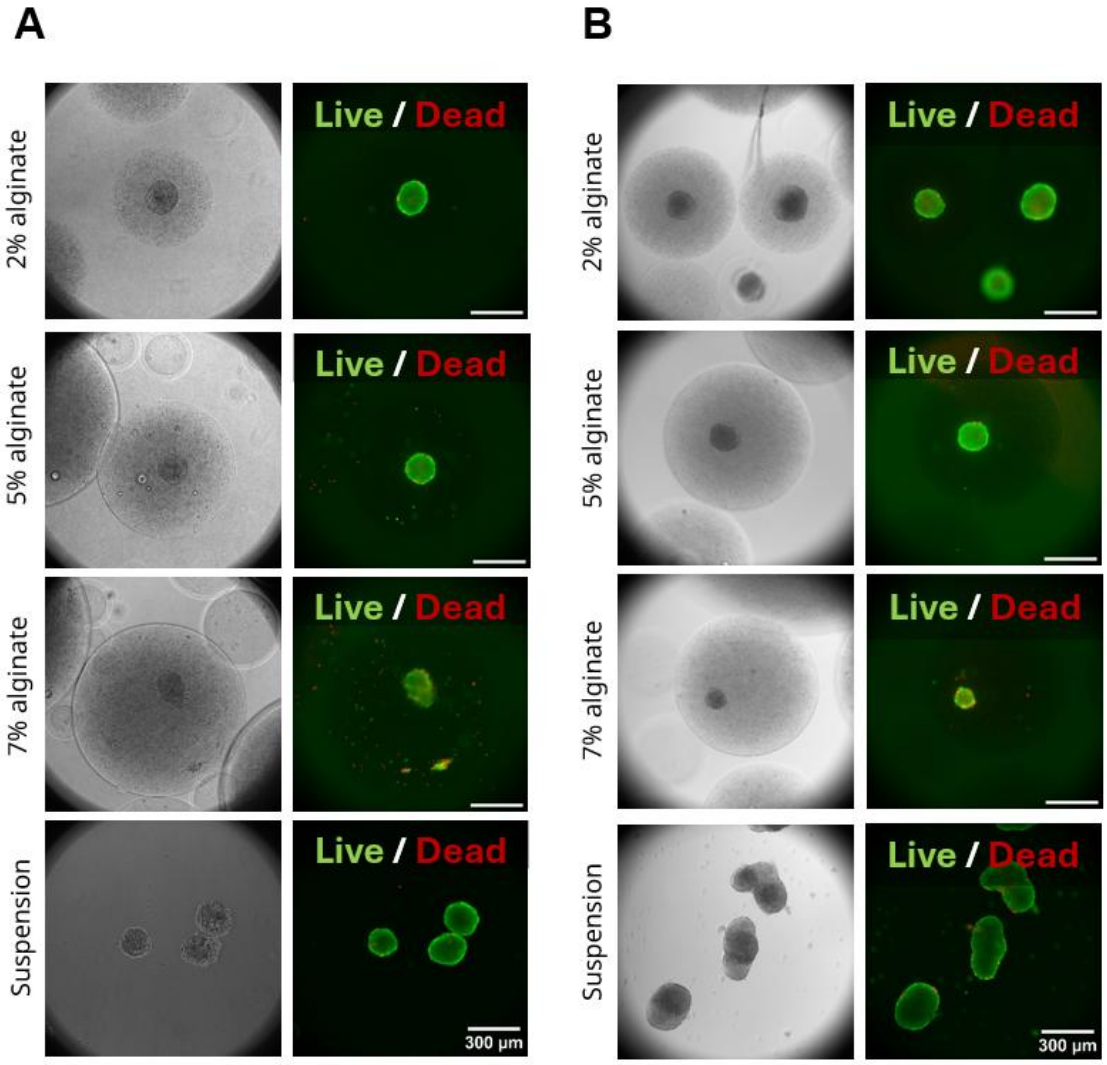

Figure 7. Fluorescence images of Live/Dead staining using Calcein-AM (Green) and Propidium Iodide (Red). **(A)** Live/Dead staining of stage 6 Day 7 immature SC-islets, 24 hours post-encapsulation. **(B)** Live/Dead staining of stage 7 Day 25 maturing SC-islets, 25 days post-encapsulation.

Fusion of clusters, leading to a significant increase in SC-islet size, could hinder mass transfer at the center of the structure causing cell loss. To assess this, the volume of the aggregates was measured both before encapsulation and after the maturation stage (25 days post-encapsulation). The SC-islets were recovered by degelling the alginate capsules. Additionally, brightfield images were captured and analyzed using ImageJ software. Figure 8 displays the size distribution for all the different conditions. Contrary to non-encapsulated controls, the size of the clusters before and after immobilized culture remained similar, due to the capsule preventing the fusion of the aggregates.

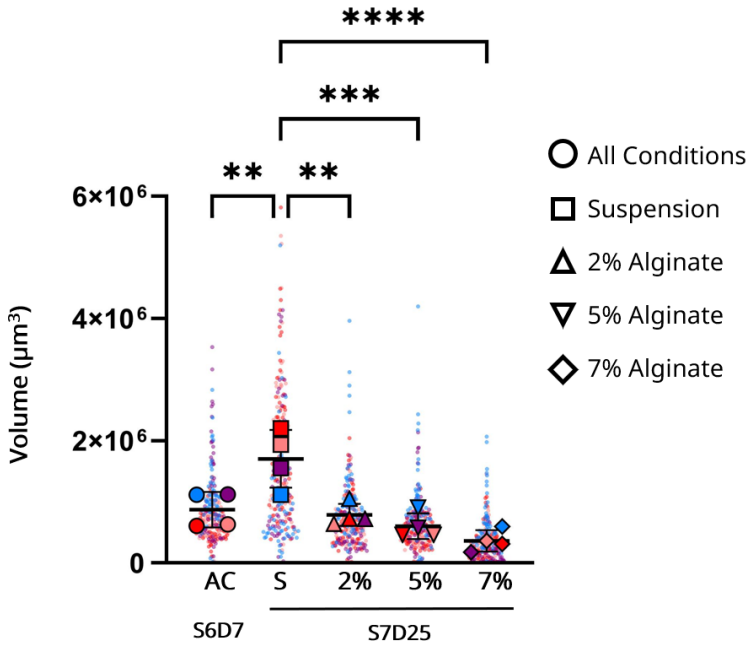

Figure 8. Cluster size distribution before encapsulation (S6D7), and 25 days after encapsulation (S7D25) (Aggregates recovered from degelled beads). Statistical significance was determined by one-way ANOVA with Tukey's multiple comparisons test (N=4, n=60). **p < 0.01, ***p < 0.001, ****p < 0.001. S6D7 = stage 6 day 7, S7D25 = stage 7 day 25

5.3.2. Maturing SC-islets characterization

To evaluate if the encapsulation microenvironment had an impact on the maturation of SC-islets, the expression of several pancreatic markers was assessed: glucagon (associated with alpha-cells), C-peptide (associated with beta-cells), NEUROD1, NKX6.1, and PDX1 (key transcription factors involve in the development and functionality of different endocrine cells which comprise the islets of Langerhans [92]). Figure 9A illustrates that increased microenvironment stiffness promotes the differentiation of alpha-cells, with a significantly higher presence of glucagon-positive alpha-cells in clusters immobilized in 7% alginate compared to those in 2% alginate or non-encapsulated SC-islets. Conversely, the differentiation of beta-cells, as indicated by C-peptide expression, and the expression of NKX6.1 were favored in non-encapsulated environments, which had lower stiffness, compared to the high-stiffness environment (7% alginate). The expression of other pancreatic markers, NEUROD1 and PDX1, remained consistent across all conditions.

The functionality of the maturing SC-islets was evaluated *in vitro* through a static glucose-stimulated insulin secretion assay, with the results presented in Figure 9B. As expected, SC-islets showed increased insulin secretion in response to glucose, with those immobilized in softer environments exhibiting higher levels of insulin secretion.

Additionally, the insulin stimulation index (ISI)—calculated as the ratio of insulin secreted in response to high glucose exposure (16 mM) relative to the average insulin secretion in response to both low glucose exposures (2 mM)—revealed no significant differences between conditions (Figure 9C). The average ISI values ranged from 2.06 to 2.57 across all conditions. These findings suggest that encapsulation did not impair the functionality of the SC-islet clusters.

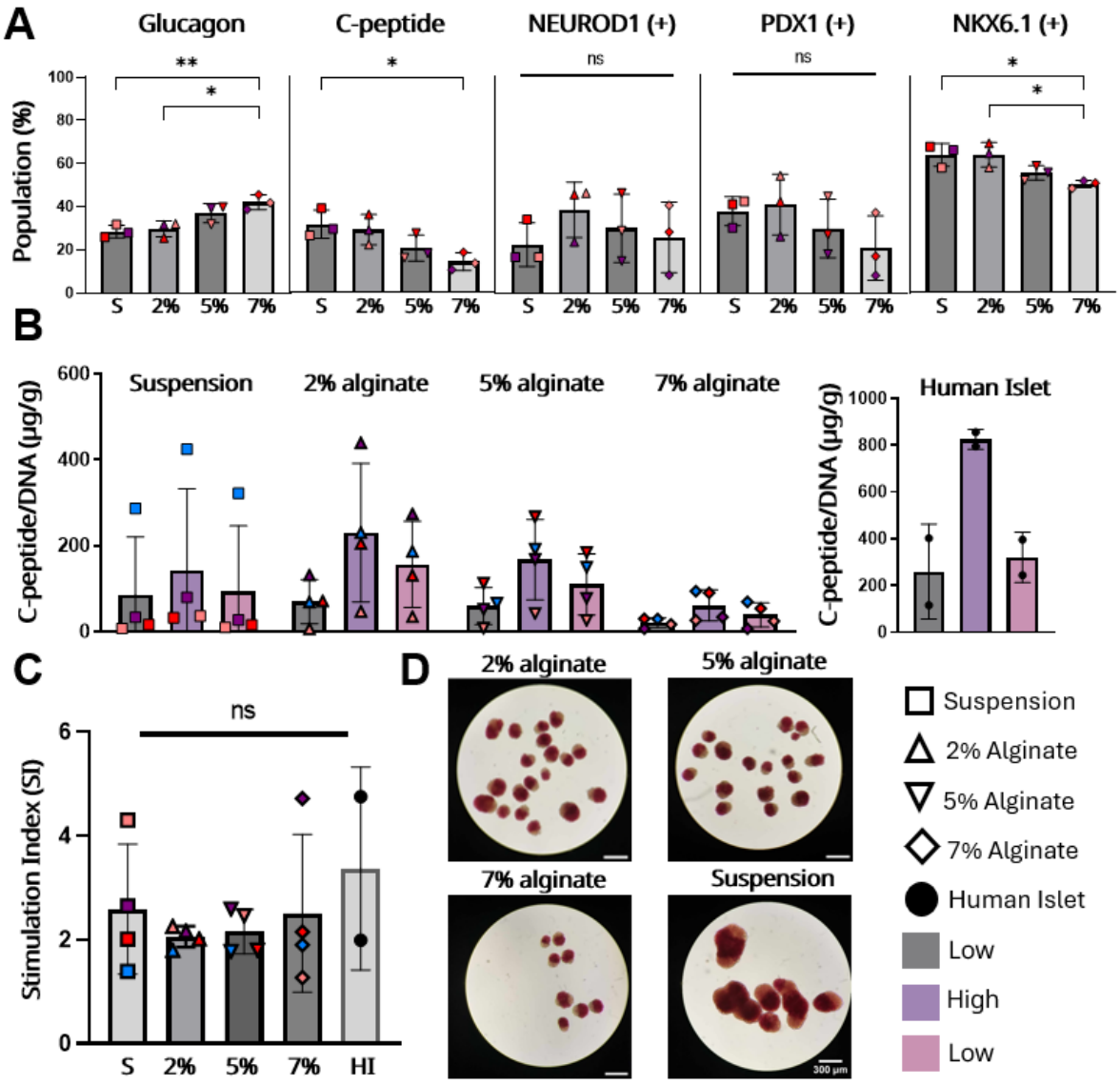

Figure 9. Characterization of S7D25 aggregates. **(A)** Flow cytometry analysis of pancreatic marker expression at stage 7 (day 25) of maturation. Statistical significance was determined by one- way Anova and Turkey's multiple comparisons test (for Glucagon, C-peptide, NKX6.1, PDX1), and Kruskal-Wallis for NEURO1 with Dunn's multiple comparison test (N=3). **(B)** Static Glucose-Stimulated Insulin Secretion (GSIS) of mature SC-islets after 3 weeks of culture in alginate beads with varying alginate concentrations (cells encapsulated at stage 6 day 7) (N=4). **(C)** Stimulation Index of maturing SC-Islets after 3 weeks of encapsulation. Statistical not significance was determined by one-way ANOVA with Tukey's multiple comparisons test (N=4). **(D)** Dithizone staining of maturing SC-islets, encapsulated and non-encapsulated after 3 weeks culture at different alginate concentrations (aggregates recovered from degelled beads)

However, when compared to human islets, the SC-islets displayed a lower insulin secretion response, indicating that while the necessary machinery for insulin secretion is present in these stem cell-derived clusters, they are still in a relatively immature state compared to fully mature human islets. The SC-islets immobilized in 7% alginate beads exhibited a lower insulin secretion response compared to the other conditions. This diminished response correlates with the lower fraction of beta cells present in these beads after 25 days (Figure 9A).

To further characterize the SC-islets, a dithizone (DTZ) staining was performed (Figure 9D). DTZ is a zinc-chelating agent that binds to the Zn^{2+} ions in the insulin secretory granules, selectively staining them a crimson red color [25].

5.4. Scale-up feasibility of encapsulated SC-islet cultured in 100 mL PBS mini bioreactors

As a proof-of-concept (n=2), we study whether the encapsulation method enables the scale-up process by protecting the SC-islets from the mechanical stress caused by the impeller. Upon analyzing the data presented before, no statistically significant differences were observed in the expression of pancreatic markers or the functionality of the SC-islets immobilized in 2% alginate compared to those in 5% alginate. With the intent of potentially transplanting the encapsulated SC-islets post-culture [4], 5% alginate was applied in these experiments.

5.4.1. Maturation of encapsulated SC-islets in vertical wheel bioreactors

As cell aggregates increase in size, they may experience mass transfer limitations at the core, leading to the formation of morphogen gradients and increased cell loss. Additionally, shear stress generated by the impeller can further contribute to a decline in cell viability [53]. To assess the impact of encapsulation on cell recovery after 25 days in culture, stage 6 Day 7 SC-islets were

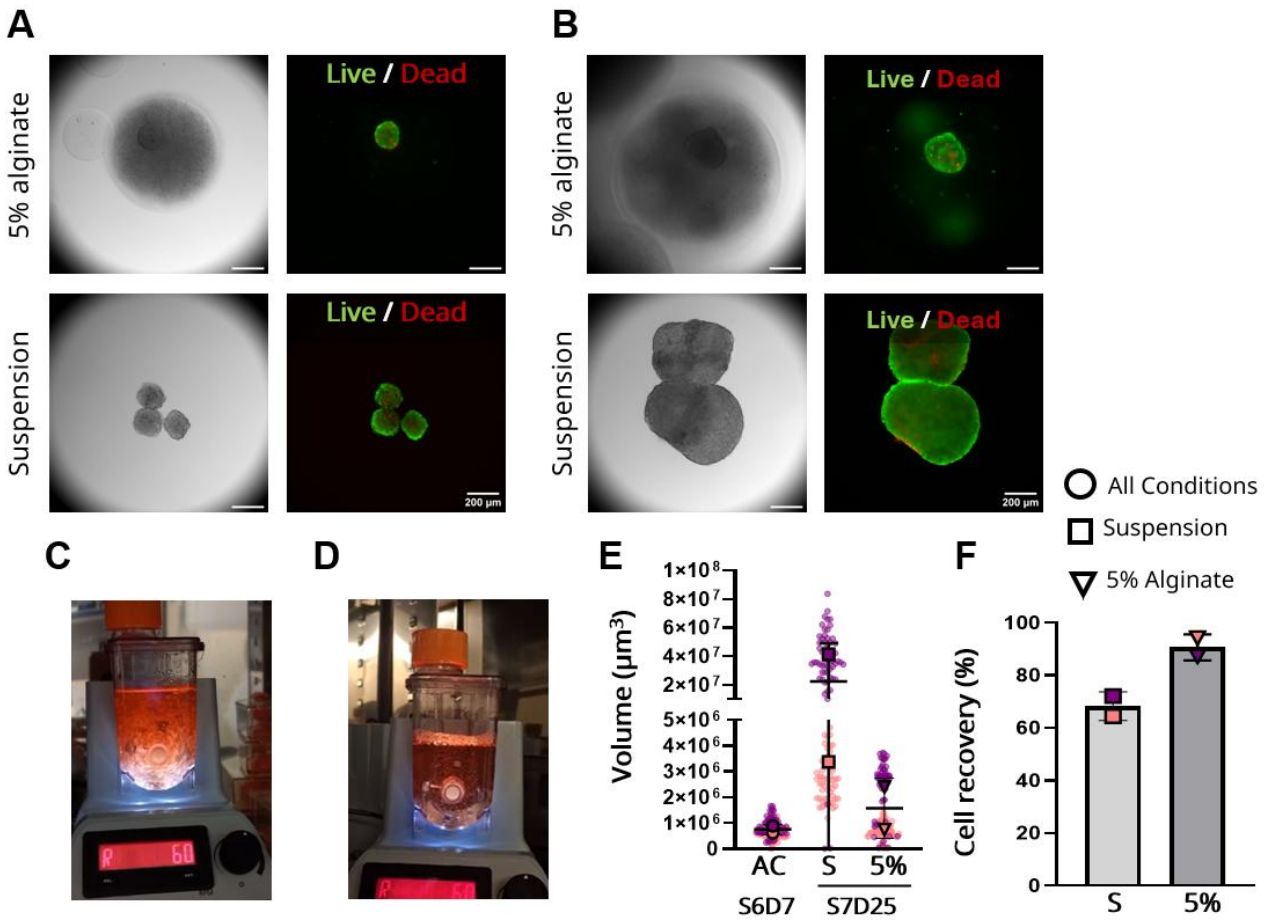

Figure 10. 25-Day Culture in PBS Mini-Bioreactor. **(A)** Live/Dead staining of stage 6 Day 7 immature SC-islets, 24 hours post-encapsulation. **(B)** Live/Dead staining of stage 7 Day 25 maturing SC-islets, 25 days post-encapsulation in 100 mL PBS mini-bioreactor culture. **(C-D)** Encapsulated and non-encapsulated SC-islets cultured in the 100 mL PBS mini bioreactor, respectively. **(E)** Cluster size distribution before encapsulation (S6D7) and 25 days post-encapsulation in 100 mL PBS mini-bioreactor culture (aggregates recovered from degelled beads). **(F)** Percentage of cell recovery after 25 days post-encapsulation

immobilized in 5% alginate using an emulsion-based encapsulation method. Both encapsulated and non-encapsulated clusters were inoculated into 100 mL PBS Mini bioreactors at a cell concentration of 1.5–2.0 × 10^5 cells/mL, and agitated at 60 rpm (following a previous published study [53]). We chose this vertical wheel bioreactor because it combines both radial and axial flow,

creating a low-shear stress environment by ensuring a more uniform energy dissipation distribution [93].

Viability was evaluated 24 h and 25 days post-encapsulation using Live/Dead staining with calcein-AM and propidium iodide (Figure 10A). Results indicated that cell viability remained high both before and after encapsulation in 5% alginate. Similarly, non-encapsulated clusters maintained high viability. Moreover, a noticeable increase in the size of non-encapsulated clusters was observed, from an average volume of $7.59x10^5$ μm^3 before encapsulation to an average volume of $2.23x10^7$ μm^3, compared to immobilized aggregates (average volume = $1.58x10^6$ μm^3) (Figure 10E). Encapsulation helped maintain a more uniform cluster size over time, by preventing aggregate fusion. Additionally, non-encapsulated clusters exhibited a lower recovery rate (~68%) compared to encapsulated clusters (~90%), likely due to increased exposure to shear stress, leading to higher cell loss.

The maturation of stage 7 day 25 SC-islets was assessed by analyzing the expression of key pancreatic markers (C-peptide, glucagon, NKX6.1, and PDX1), their functionality (static glucose-stimulated insulin secretion), and insulin storage (dithizone staining), as shown in Figure 11. Flow cytometry data revealed that C-peptide expression remained consistent (~20%) across both conditions. Interestingly, the transcription factor PDX1 exhibited lower expression in both encapsulated and non-encapsulated clusters compared to cultures maintained in ultralow attachment plates on a Celltron orbital shaker at 100 rpm. Pancreatic and duodenal homeobox 1 (PDX1) is a transcription factor involve in the pancreatic development and mature beta-cell function [94]. Low expression of this transcription factor may suggest certain immaturity of the beta-cells [95].

Mature beta-cells secrete insulin in response to glucose stimulation [96]. Insulin release is triggered by the uptake and oxidation of glucose within pancreatic beta-cells. At low glucose concentrations, human beta-cells remain hyperpolarized. However, at high glucose levels, ATP-sensitive potassium channels close due to increase in ATP production, leading to cell depolarization. This process induces an influx of intracellular calcium ions (Ca^{2+}) through voltage-dependent calcium channels, ultimately triggering the exocytosis of insulin stored in secretory granules [97,98].

In this study, encapsulated and non-encapsulated stem-cell-derived (SC) pancreatic islets were differentiated and matured for 25 days in 100 mL PBS mini-bioreactors. Their functionality was assessed by exposure to low (2.8 mM) and high (16 mM) glucose concentrations. Both immobilized and non-immobilized SC-islets secreted insulin in proportion to glucose levels. Notably, non-encapsulated SC-islets cultured in the mini-bioreactor exhibited a stronger insulin response compared to those cultured in standard plates. In contrast, encapsulated SC-islets showed a lower insulin secretion response. It is important to note that these results were standardized based on DNA content. In the encapsulated condition, the DNA from dead cells remained trapped in the beads, while in suspension, the DNA from dead cells was removed during medium exchanges. This may have led to a less accurate DNA measurement, which could explain the observed differences. Further, diffusional limitation of the different molecules evaluated in the assay (glucose and C-peptide) could also have influenced these differences.

Additionally, Figure 11D shows the dithizone staining of the encapsulated and non-encapsulated SC-islets, alongside human islets, to assess the presence of insulin secretory granules. Despite the relatively low expression of the transcription factor PDX1, the SC-islets demonstrated key characteristics of mature islets when challenged with low (2.8 mM) and high (16 mM) glucose

concentrations. These findings suggest that the mini-bioreactor system may enhance non-immobilized SC-islet function and maturation.

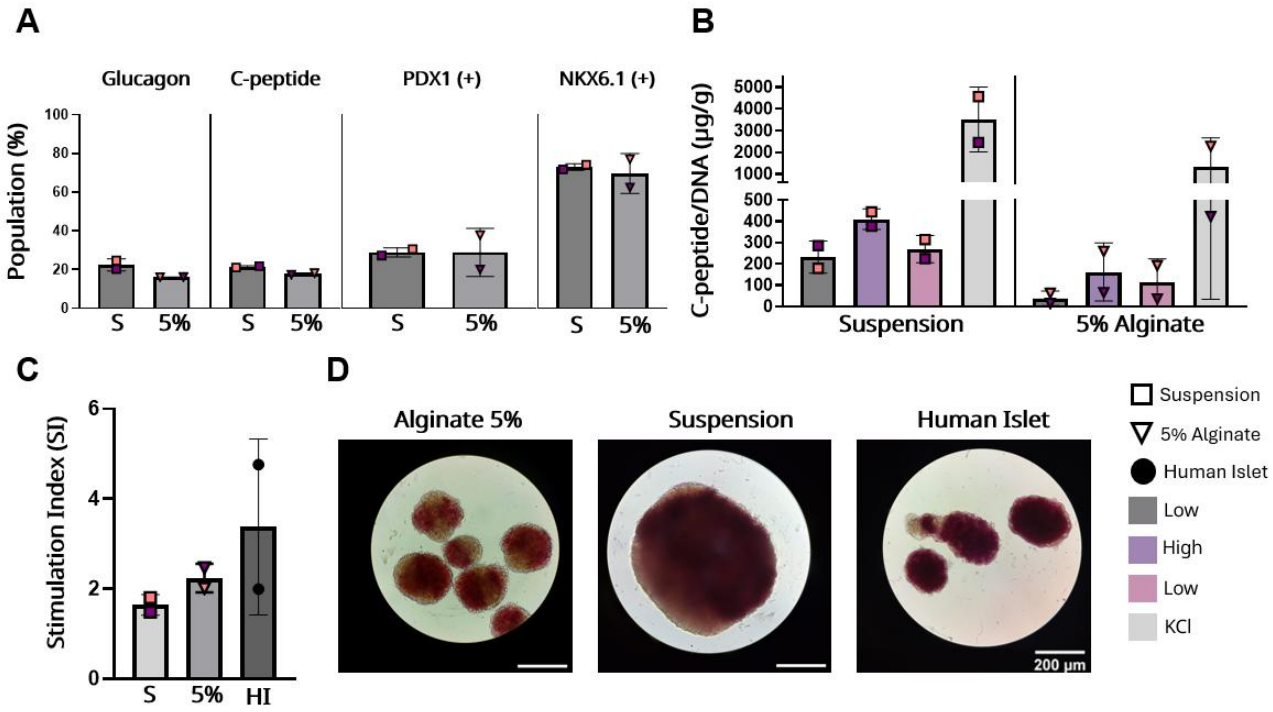

Figure 11. Characterization of S7D25 aggregates culture 25 days in 100 mL PBS mini bioreactors. **(A)** Flow cytometry analysis of pancreatic marker expression at stage 7 day 25 of maturation (N=2). **(B)** Static Glucose-Stimulated Insulin Secretion (GSIS) of maturing SC-islets after 3 weeks of culture in vertical wheel bioreactor (N=2). **(C)** Stimulation Index of maturing SC-Islets after 3 weeks of culture (N=2) and human islets. **(D)** Dithizone staining of maturing SC-islets, non encapsulated, and encapsulated after 3 weeks of culture in the PBS mini bioreactor (aggregates recovered from degelled beads) (N=2). Human islets were used as a control

6. Discussion

In this project, we investigate the impact of microenvironment stiffness on the composition and functionality of stem cell-derived pancreatic islets by maturing them in an immobilized environment with varying alginate concentrations (2%, 5%, and 7%). Additionally, we assess whether microencapsulation can prevent the agglomeration of stem cell-derived pancreatic islets and influence local energy dissipation rates. We successfully immobilized immature SC-islets using an emulsion-based encapsulation technique. This approach prevented cluster agglomeration, resulting in a high cell recovery yield (90 ± 4.9%) after 25 days of culture in a vertical wheel bioreactor. This high yield could enable the production of clinically relevant cell quantities, potentially allowing treatment for multiple patients. Furthermore, we achieved *in vitro* maturation of both immobilized and non-immobilized SC-islets, cultured in downscaled stirred suspension and vertical wheel bioreactors. Our findings suggest that alginate concentration influences endocrine specification, likely through mechanical signaling or molecular diffusion. These insights may provide valuable guidance for optimizing hydrogel stiffness in transplantation devices.

We first aimed to optimize the seeding density of pancreatic progenitor cells during the aggregation process. Our data showed no significant differences in cell identity or cell recovery rates among seeding densities of 500, 1000, 1500 cells/microwell. However, studies suggest that in 3D cultures, the size of pluripotent stem cell aggregates can influence cell fate during differentiation, as observed in cardiomyocyte lineage development [99,100]. This highlights the potential impact of aggregate size at earlier stages of the differentiation protocol.

The mechanical stability of the beads plays an important role in the cell transplantation. These capsules must be strong enough to withstand the transplantation procedure and

transplantation site shear forces [101]. Figure 6 presents the mechanical properties of the 2%, 5%, and 7% alginate beads, highlighting their response to compression. Interestingly, all three formulations exhibited a plastic behaviour at 10% compressive volume, indicating irreversible and inelastic matrix deformation due to the mechanical disruption of intermolecular bonds [102]. At 30% compressive volume, the average Young's modulus of our beads was 5.3 kPa, 28.8 kPa, and 41.8 kPa for 2%, 5%, and 7% alginate beads, respectively. This trend can be attributed to the higher degree of cross-linking structures formed in denser alginate matrices. The physiological stiffness of the subcutaneous cavity, a typical site for islet transplantation, ranges from 15-34 kPa [103]. A transplantation device with stiffness similar to that of the transplantation site could reduce mechanical stress [104].

Several studies suggest that culturing pluripotent stem cells (PSCs) in a 3D microenvironment using hydrogel encapsulation can enhance differentiation efficiency compared to traditional 2D culture systems [105–107]. The 3D microenvironment offers both biochemical and biophysical cues that closely mimic the physiological conditions of embryonic development [108]. Various research groups have enhanced these hydrogels by modifying their viscoelastic properties and incorporating extracellular matrix (ECM) components into their structure. These ECM components can include collagen, fibronectin, and peptides such as arginine-glycine-aspartate (RGD) [109,110]. The addition of ECMs to the hydrogel surface enables interactions with transmembrane receptors on the cell clusters, particularly integrins. These receptors play a crucial role in sensing mechanical changes within the microenvironment and converting extracellular mechanical stimuli into intracellular signaling pathways, which are essential for cell behavior and function[82,83]. It is important to note that encapsulated cells can also secrete ECM. Therefore, the presence of these macromolecules is not exclusive to modified hydrogels. In our study, we

observed that SC-islets cultured in a high-stiffness environment (7% alginate) exhibited a significantly higher proportion of glucagon-producing alpha-cells compared to non-encapsulated pancreatic clusters and softer environments (2% alginate). Interestingly, the opposite trend was observed for insulin-producing beta-cells and the expression of the pancreatic marker NKX6.1. Non-encapsulated cultures promoted greater differentiation into pancreatic beta-cells, whereas stiffer microenvironments resulted in a lower beta-cell yield.

Pre-alpha-cells express the transcription factors ARX, IRX2, and ARX, but they do not express key beta-cell markers such as PDX1 and NKX6.1. Additionally, studies suggest that the precursors of pre-alpha-cells originate from NKX6.1-negative cells [111]. This aligns with the findings of the present study, where SC-islets immobilized in 7% alginate, which contained a higher proportion of glucagon-producing alpha-cells, exhibited lower levels of PDX1 and NKX6.1. PDX1 is a crucial transcription factor involved in beta-cell maturation and the regulation of insulin secretion, while NKX6.1 plays a vital role in beta-cell function and proliferation. The co-expression of these two transcription factors in pancreatic progenitors may signifies a commitment toward the mono-hormonal insulin-producing beta-cell lineage [112]. The reduced expression of PDX1 and NKX6.1 in SC-islets encapsulated in 7% alginate may explain their lower insulin secretion in the static glucose-stimulated insulin assay. Despite all conditions (SC-islets maturated in 2%, 5%, and 7% alginate beads) showing some insulin release in response to varying glucose concentrations—indicating that the aggregates possess the basic machinery to sense glucose fluxes—the insulin secretion levels were lower when compared to human islets. Indication that the SC-islets still exhibit some signs of immaturity.

Furthermore, the differences observed in the characterization of SC-islets matured at varying alginate concentrations could be attributed to differences in oxygen and nutrient diffusion.

Oxygen (O_2) plays a crucial role in organ development and cellular homeostasis. The partial pressure of O_2 (pO_2) is involved in the pancreatic development. During the early stages of embryonic pancreatic development, oxygen levels are low due to limited vascularization. In later stages, increased blood flow raises oxygen levels, which promotes endocrine differentiation [113,114]. Hakim *et al.* [113] reported that high O_2 concentrations activate the Wnt signaling pathway, which induces the differentiation of definitive endoderm cells into pancreatic progenitors [115]. Additionality, Cechin et al. [116] demonstrated that pO_2 modulation plays a crucial role in the differentiation of insulin-producing beta-cells under *in vivo* conditions. Half of the diabetic mice transplanted with pancreatic progenitor cells restored normoglycemic levels after being treated with post-transplantation hyperbaric oxygen, whereas none of the mice not subjected to this treatment experienced a reversal of diabetes.

Significant cell loss (31.72 ± 3.86%) was observed in the PBS mini bioreactor culture of non-encapsulated SC-islets, compared to the immobilized cluster (9.33 ± 3.50%). This loss may be attributed to the significant increase in the size of the non-encapsulated clusters, which could lead to mass transfer limitations [53]. In contrast, the encapsulating capsule protected the aggregates from shear stress caused by the impeller. When comparing the identity of encapsulated and non-encapsulated SC-islets, pancreatic markers remained consistent across both conditions. However, functional assessments showed that non-encapsulated SC-islets exhibited higher insulin secretion than encapsulated aggregates (Figure 11). These results were normalized based on total DNA content. In the encapsulated condition, DNA from dead cells remained trapped in the beads, whereas in suspension, DNA from dead cells was removed during medium exchanges. Both immobilized and non-immobilized SC-islets had a good response when challenge to different glucose concentrations. However, the increase in insulin secretion seen may not be entirely

accurate due to the normalization technique used. To improve accuracy, an alternative normalization method, such as total protein quantification, is recommended. It is important to note that this section of the study was a proof of concept with a sample size of N=2. Further experiments are needed to confirm these findings and ensure reproducibility.

The efficient encapsulation of SC-islets in high-alginate concentrations was successfully achieved using emulsion-based encapsulation, a method that offers high throughput and relatively low shear stress. By minimizing mechanical stress during encapsulation, this method enhances cell viability and supports SC-islet maturation.

A key advantage of the emulsion-based approach is its ability to generate large quantities of beads within just 20–30 minutes, a significant improvement over nozzle-based methods, which typically have an extrusion throughput of approximately 10 to 360 mL/h [68]. Moreover, encapsulation plays a crucial role in the biomanufacturing pipeline by controlling the SC-islet size, preventing cluster aggregation, and reduced shear-induced cell damage, makes this technique highly suitable for large-scale cell encapsulation and bioprocessing.

After the production of SC-islets, we envisioned the transplantation of the encapsulated clusters into animal models to further investigate the preservation of functionality in an *in vivo* environment. The alginate composition used for the emulsion-based encapsulation process consisted of a 50:50 mixture of low-viscosity sodium alginate (LVM) and medium-viscosity sodium alginate (MVG), both containing ≥60% guluronate monomer units. This alginate formulation was selected based on the study previously published by Hoesli, *et al*. [64], which demonstrated low fibrotic overgrowth and low antibody permeability. These properties enhance the reproducibility of the present study's findings, making them suitable for preclinical applications.

This study has certain limitations. First, the aggregation method using AggreWell™ 400 6-well plate is not scalable. The sensitivity of the clusters to dislodging from the microwells during media changes or when transporting plates from the incubator to the biosafety cabinet (BSC) increases the risk of cell loss. Furthermore, the adherent differentiation method used up to Stage 4 lacks scalability. There is a high variability between batches, and the high manipulation of the culture plate increases the risk of contamination. To address these challenges, a 3D suspension culture using a vertical-wheel or stirred bioreactor is recommended [52,53]. Additionally, pluripotent stem cell expansion should be performed in a perfusion bioreactor, as the continuous influx of nutrients can promote cell proliferation and maintain pluripotency [117].

The size of the clusters should be optimized. It's been reported in multiple studies that the size of the human stem cells aggregates before the start of the endocrine differentiation has a huge impact on the differentiation outcome. Furthermore, it's been reported the 3D microenvironment using hydrogel encapsulation can enhance differentiation efficiency compared to traditional 2D culture systems [105–107]. For further studies, it would be recommended to encapsulate the pluripotent clusters and performing the pancreatic differentiation within the capsule microenvironment.

The underlying mechanism behind the increased production of insulin-producing cells in softer environments and the higher prevalence of glucagon-producing cells in stiffer environments remains unclear. To gain deeper insights, RNA sequencing (RNA-seq) analysis is recommended to identify differentially expressed genes and determine which pathways are upregulated or downregulated. This approach could provide greater clarity on how mechanical stimuli within the microenvironment influence cellular differentiation by activating or inhibiting specific pathways.

7. Conclusions

SC-islets hold significant promise in the field of regenerative medicine, emerging as a potentially unlimited source for transplantation. However, scaling up suspension cultures of SC-islets is challenging due to issues such as agglomeration in low-shear areas and cell damage in high-shear areas. To address these limitations, SC-islets can be encapsulated in hydrogels. The capsule not only provides protection against mechanical stress caused by bioreactor impellers, reducing agglomeration, but also offers potential immunoprotection during transplantation while allowing bidirectional nutrient diffusion.

In this study, we (1) investigated the impact of seeding density of endocrine precursor cells during cluster formation on the differentiation of SC-islets. Our findings indicated that seeding densities of 500, 1000, and 1500 cells per microwell had no significant effect on the identity, maturation, or cell recovery by day 10 of stage 7. (2) We also examined the effect of 2%, 5%, and 7% alginate concentrations in the encapsulation process on SC-islet differentiation. Our results suggested that matrix stiffness plays a critical role in guiding pancreatic cell fate. Stiffer environments promoted alpha-cell differentiation, while softer or non-encapsulated conditions favored beta-cell maturation. These findings underscore the importance of mechanical properties in optimizing differentiation protocols for pancreatic lineage commitment. (3) As proof-of-concept, we demonstrated the feasibility of using an emulsion-based encapsulation method to protect SC-islets from mechanical stress caused by the impeller, achieving a high cell recovery rate (~90%).

Overall, the mechanisms underlying the influence of microenvironment stiffness on glucagon-producing alpha-cells and insulin-producing beta-cells remain underexplored. This

knowledge gap presents an opportunity for future studies aimed at enhancing SC-islet maturation and identity, as well as optimizing *in vitro* maturation protocols by targeting mechanotransduction pathways.

8. References

1. Cayabyab, F., Nih, L. R. & Yoshihara, E. Advances in Pancreatic Islet Transplantation Sites for the Treatment of Diabetes. *Front. Endocrinol. (Lausanne).* **12**, (2021).

2. Velazco-Cruz, L. *et al.* Acquisition of Dynamic Function in Human Stem Cell-Derived β Cells. *Stem Cell Reports* **12**, 351–365 (2019).

3. Paez-Mayorga, J. *et al.* Emerging strategies for beta cell transplantation to treat diabetes. *Trends Pharmacol. Sci.* **43**, 221–233 (2022).

4. Keymeulen, B. *et al.* Encapsulated stem cell–derived β cells exert glucose control in patients with type 1 diabetes. *Nat. Biotechnol.* **42**, (2023).

5. Thakur, G. *et al.* Scaffold-free 3D culturing enhance pluripotency, immunomodulatory factors, and differentiation potential of Wharton's jelly-mesenchymal stem cells. *Eur. J. Cell Biol.* **101**, (2022).

6. Cohen, P. J. R. *et al.* Engineering 3D micro-compartments for highly efficient and scale-independent expansion of human pluripotent stem cells in bioreactors. *Biomaterials* **295**, (2023).

7. Fattahi, P. *et al.* Core–shell hydrogel microcapsules enable formation of human pluripotent stem cell spheroids and their cultivation in a stirred bioreactor. *Sci. Rep.* **11**, 1–13 (2021).

8. Coyle, M. & Kulendran, M. Anatomy of the pancreas and spleen. *Surg. (United Kingdom)* **40**, 213–218 (2022).

9. Shelat, V. G. & Kapoor, V. K. *Pancreas; Anatomy and Development*. *Encyclopedia of*

Gastroenterology, Second Edition (Elsevier Inc., 2019). doi:10.1016/B978-0-12-801238-3.65873-7.

10. Leung, P. S. & Ip, S. P. Pancreatic acinar cell: Its role in acute pancreatitis. *Int. J. Biochem. Cell Biol.* **38**, 1024–1030 (2006).

11. Logsdon, C. D. & Ji, B. The role of protein synthesis and digestive enzymes in acinar cell injury. *Nat. Rev. Gastroenterol. Hepatol.* **10**, 362–370 (2013).

12. Otter, S. & Lammert, E. Exciting Times for Pancreatic Islets: Glutamate Signaling in Endocrine Cells. *Trends Endocrinol. Metab.* **27**, 177–188 (2016).

13. Ionescu-Tirgoviste, C. *et al.* A 3D map of the islet routes throughout the healthy human pancreas. *Sci. Rep.* **5**, 1–14 (2015).

14. Gromada, J., Franklin, I. & Wollheim, C. B. A-Cells of the Endocrine Pancreas: 35 Years of Research But the Enigma Remains. *Endocr. Rev.* **28**, 84–116 (2007).

15. Bramswig, N. C. & Kaestner, K. H. . Transcriptional regulation of α-cell differentiation. *Journalism* **11**, 369–373 (2010).

16. Wendt, A. & Eliasson, L. Pancreatic α-cells – The unsung heroes in islet function. *Semin. Cell Dev. Biol.* **103**, 41–50 (2020).

17. Svendsen, B. *et al.* Insulin Secretion Depends on Intra-islet Glucagon Signaling. *Cell Rep.* **25**, 1127-1134.e2 (2018).

18. Quesada, I., Tudurí, E., Ripoll, C. & Nadal, Á. Physiology of the pancreatic α-cell and glucagon secretion: Role in glucose homeostasis and diabetes. *J. Endocrinol.* **199**, 5–19 (2008).

19. Pisania, A. *et al.* Quantitative analysis of cell composition and purity of human pancreatic islet preparations. *Physiol. Behav.* **176**, 139–148 (2011).

20. Bartolomé, A. The Pancreatic Beta Cell: Editorial. *Biomolecules* **13**, 10–12 (2023).

21. Sugumar, V. *et al.* A Comprehensive Review of the Evolution of Insulin Development and Its Delivery Method. *Pharmaceutics* **14**, 1–28 (2022).

22. Kerper, N., Ashe, S. & Hebrok, M. Pancreatic β-Cell Development and Regeneration. *Cold Spring Harb. Perspect. Biol.* **14**, 1–20 (2022).

23. Humbel, R. E. *Biosynthesis of Insulin*. *Acta Diabetologica Latina* vol. 5 Suppl 1 (2022).

24. Li, Y. V. Zinc and insulin in pancreatic beta-cells. *Endocrine* **45**, 178–189 (2014).

25. Shiroi, A. *et al.* Identification of Insulin-Producing Cells Derived from Embryonic Stem Cells by Zinc-Chelating Dithizone. *Stem Cells* **20**, 284–292 (2002).

26. Henquin, J. C. Glucose-induced insulin secretion in isolated human islets: Does it truly reflect β-cell function in vivo? *Mol. Metab.* **48**, 1–16 (2021).

27. Nkonge, K. M., Nkonge, D. K. & Nkonge, T. N. The epidemiology, molecular pathogenesis, diagnosis, and treatment of maturity-onset diabetes of the young (MODY). *Clin. Diabetes Endocrinol.* **6**, 1–10 (2020).

28. Punthakee, Z., Goldenberg, R. & Katz, P. Definition, Classification and Diagnosis of Diabetes, Prediabetes and Metabolic Syndrome. *Can. J. Diabetes* **42**, S10–S15 (2018).

29. Eizirik, D. L., Pasquali, L. & Cnop, M. Pancreatic β-cells in type 1 and type 2 diabetes mellitus: different pathways to failure. *Nat. Rev. Endocrinol.* **16**, 349–362 (2020).

30. Mobasseri, M. *et al.* Prevalence and incidence of type 1 diabetes in the world: A systematic review and meta-analysis. *Heal. Promot. Perspect.* **10**, 98–115 (2020).

31. Ni, Q., Pham, N. B., Meng, W. S., Zhu, G. & Chen, X. Advances in immunotherapy of type I diabetes. *Adv. Drug Deliv. Rev.* **139**, 83–91 (2019).

32. Berney, T. *et al.* From islet of Langerhans transplantation to the bioartificial pancreas. *Press. Medicale* **51**, 104139 (2022).

33. Bruni, A., Gala-Lopez, B., Pepper, A. R., Abualhassan, N. S. & James Shapiro, A. M. Islet cell transplantation for the treatment of type 1 diabetes: Recent advances and future challenges. *Diabetes, Metab. Syndr. Obes.* **7**, 211–223 (2014).

34. Falcetta, P. *et al.* Insulin discovery: A pivotal point in medical history. *Metabolism.* **127**, 154941 (2022).

35. Katsarou, A. *et al.* Type 1 diabetes mellitus. *Nat. Rev. Dis. Prim.* **3**, 1–18 (2017).

36. Zhu, B., Abu Irsheed, G. M., Martyn-Nemeth, P. & Reutrakul, S. Type 1 Diabetes, Sleep, and Hypoglycemia. *Curr. Diab. Rep.* **21**, (2021).

37. Amiel, S. A. The consequences of hypoglycaemia. **64**, 963–970 (2021).

38. Jamiolkowski, R. M., Guo, L. Y., Li, Y. R., Shaffer, S. M. & Naji, A. Islet transplantation in type I diabetes mellitus. *Yale J. Biol. Med.* **85**, 37–43 (2012).

39. A. M. J. Shapiro, J. R. T. Lakey, E. A. Ryan, G. S. Korbutt, E. Toth, G. L. Warnock, et al. Islet Transplantation in Seven Patients with Type 1 Diabetes Mellitus Using a Glucocorticoid-Free Immunosuppressive Regimen. *N. Engl. J. Med.* **343**, 230–238 (2000).

40. Barton, F. B. *et al.* Improvement in outcomes of clinical islet transplantation: 1999-2010.

Diabetes Care **35**, 1436–1445 (2012).

41. Wang, X. *et al.* Engineered immunomodulatory accessory cells improve experimental allogeneic islet transplantation without immunosuppression. *Sci. Adv.* **8**, 1–17 (2022).

42. CITR Coordinating Center, The Emmes Corporation & Rockville MD. Eleventh Allograft Report. (2022).

43. Du, Y. *et al.* Human pluripotent stem-cell-derived islets ameliorate diabetes in non-human primates. *Nat. Med.* **28**, 272–282 (2022).

44. Rezania, A. *et al.* Reversal of diabetes with insulin-producing cells derived in vitro from human pluripotent stem cells. *Nat. Biotechnol.* **32**, 1121–1133 (2014).

45. Pagliuca, F. W. *et al.* Generation of functional human pancreatic β cells in vitro. *Cell* **159**, 428–439 (2014).

46. Hogrebe, N. J., Augsornworawat, P., Maxwell, K. G., Velazco-Cruz, L. & Millman, J. R. Targeting the cytoskeleton to direct pancreatic differentiation of human pluripotent stem cells. *Nat. Biotechnol.* **38**, 460–470 (2020).

47. Balboa, D. *et al.* Functional, metabolic and transcriptional maturation of human pancreatic islets derived from stem cells. *Nat. Biotechnol.* **40**, 1042–1055 (2022).

48. Russ, H. A. *et al.* Controlled induction of human pancreatic progenitors produces functional beta-like cells in vitro . *EMBO J.* **34**, 1759–1772 (2015).

49. Braam, M. J. S. *et al.* Protocol development to further differentiate and transition stem cell-derived pancreatic progenitors from a monolayer into endocrine cells in suspension culture. *Sci. Rep.* **13**, 1–17 (2023).

50. Ackermann, M. *et al.* Continuous human iPSC-macrophage mass production by suspension culture in stirred tank bioreactors. *Nat. Protoc.* **17**, 513–539 (2022).

51. Olmer, R. *et al.* Suspension culture of human pluripotent stem cells in controlled, stirred bioreactors. *Tissue Eng. - Part C Methods* **18**, 772–784 (2012).

52. Pollock, S. D., Galicia-Silva, I. M., Liu, M., Gruskin, Z. L. & Alvarez-Dominguez, J. R. Scalable generation of 3D pancreatic islet organoids from human pluripotent stem cells in suspension bioreactors. *STAR Protoc.* **4**, 102580 (2023).

53. Iworima, D. G. *et al.* Metabolic switching, growth kinetics and cell yields in the scalable manufacture of stem cell-derived insulin-producing cells. *Stem Cell Res. Ther.* **15**, 1–28 (2024).

54. Parent, A. V. *et al.* Development of a scalable method to isolate subsets of stem cell-derived pancreatic islet cells. *Stem Cell Reports* **17**, 979–992 (2022).

55. Komatsu, H. *et al.* Oxygen environment and islet size are the primary limiting factors of isolated pancreatic islet survival. *PLoS One* **12**, 1–17 (2017).

56. Iworima, D. G. *et al.* Metabolic switching, growth kinetics and cell yields in the scalable manufacture of stem cell-derived insulin-producing cells. *Stem Cell Res. Ther.* **15**, 1 (2024).

57. Torizal, F. G. *et al.* Production of homogenous size-controlled human induced pluripotent stem cell aggregates using ring-shaped culture vessel. *J. Tissue Eng. Regen. Med.* **16**, 254–266 (2022).

58. Zhang, Q. *et al.* Islet Encapsulation: New Developments for the Treatment of Type 1

Diabetes. *Front. Immunol.* **13**, 1–16 (2022).

59. Hogrebe, N. J., Ishahak, M. & Millman, J. R. Developments in stem cell-derived islet replacement therapy for treating type 1 diabetes. *Cell Stem Cell* **30**, 530–548 (2023).

60. Prüsse, U. *et al.* Comparison of different technologies for alginate beads production. *Chem. Pap.* **62**, 364–374 (2008).

61. Vorlop, K.-D. & Klein, J. New Developments in the Field of Cell Immobilization — Formation of Biocatalysts by Ionotropic Gelation. *Enzym. Technol.* 219–235 (1983) doi:10.1007/978-3-642-69148-5_20.

62. Lewińska, D., Rosiński, S. & Weryński, A. Influence of Process Conditions during Impulsed Electrostatic Droplet Formation on Size Distribution of Hydrogel Beads. *Artif. Cells. Blood Substit. Immobil. Biotechnol.* **32**, 41–53 (2004).

63. Moeun, B. N. *et al. Islet Encapsulation: A Long-Term Treatment for Type 1 Diabetes*. *Encyclopedia of Tissue Engineering and Regenerative Medicine* vols 1–3 (Elsevier, 2019).

64. Hoesli, C. A. *et al.* Reversal of diabetes by βtC3 cells encapsulated in alginate beads generated by emulsion and internal gelation. *J. Biomed. Mater. Res. - Part B Appl. Biomater.* **100 B**, 1017–1028 (2012).

65. Ozbolat, I. T. & Yu, Y. Bioprinting toward organ fabrication: Challenges and future trends. *IEEE Trans. Biomed. Eng.* **60**, 691–699 (2013).

66. Poncelet, D. *et al.* Production of alginate beads by emulsification/internal gelation. I. Methodology. *Appl. Microbiol. Biotechnol.* **38**, 39–45 (1992).

67. Chan, L. W., Lee, H. Y. & Heng, P. W. S. Mechanisms of external and internal gelation

and their impact on the functions of alginate as a coat and delivery system. *Carbohydr. Polym.* **63**, 176–187 (2006).

68. Hoesli, C. A. *et al.* Pancreatic cell immobilization in alginate beads produced by emulsion and internal gelation. *Biotechnol. Bioeng.* **108**, 424–434 (2011).

69. Shu, J., McClements, D. J., Luo, S., Ye, J. & Liu, C. Effect of internal and external gelation on the physical properties, water distribution, and lycopene encapsulation properties of alginate-based emulsion gels. *Food Hydrocoll.* **139**, 108499 (2023).

70. Alipour, M. & Aghazadeh, M. *Cell Microencapsulation*. *Principles of Biomaterials Encapsulation: Volume One* (Elsevier Ltd., 2023). doi:10.1016/B978-0-323-85947-9.00005-4.

71. Calafiore, R. & Basta, G. Clinical application of microencapsulated islets : Actual prospectives on progress and challenges ☆. **68**, 84–92 (2014).

72. Bochenek, M. A. *et al.* Alginate encapsulation as long-term immune protection of allogeneic pancreatic islet cells transplanted into the omental bursa of macaques. doi:10.1038/s41551-018-0275-1.

73. Basta, G. *et al.* Long-term metabolic and immunological follow-up of nonimmunosuppressed patients with type 1 diabetes treated with microencapsulated islet allografts: Four cases. *Diabetes Care* **34**, 2406–2409 (2011).

74. Jacobs-Tulleneers-Thevissen, D. *et al.* Sustained function of alginate-encapsulated human islet cell implants in the peritoneal cavity of mice leading to a pilot study in a type 1 diabetic patient. *Diabetologia* **56**, 1605–1614 (2013).

75. Ghoneim, M. A., Gabr, M. M., El-Halawani, S. M. & Refaie, A. F. Current status of stem cell therapy for type 1 diabetes: a critique and a prospective consideration. *Stem Cell Res. Ther.* **15**, 1–13 (2024).

76. Ramzy, A. *et al.* Implanted pluripotent stem-cell-derived pancreatic endoderm cells secrete glucose-responsive C-peptide in patients with type 1 diabetes. *Cell Stem Cell* **28**, 2047-2061.e5 (2021).

77. Vertex, A. M., After, T. P., Deaths, U. P., Collab, C. & Next, E. Vertex T1D Trial Paused After 2 Unrelated Patient Deaths , CRISPR Collab Ends Next Day. 1–11 https://www.thejdca.org/publications/report-library/archived-reports/2024-reports/vertex-t1d-trial-paused-after-2-unrelated-patient-deaths-crispr-collab-ends-next-day.html#:~:text=Vertex pauses VX-880 T1D,with most being insulin independent (2024).

78. Library, R. Vertex T1D Trial Moves into Phase III. 1–10 https://www.thejdca.org/publications/report-library/archived-reports/2024-reports/vertex-t1d-trial-moves-into-phase-iii.html#:~:text=The VX-880 trial utilizes,trial was cleared to resume (2025).

79. Details, P. R. Vertex Announces Program Updates for Type 1 Diabetes Portfolio. https://investors.vrtx.com/news-releases/news-release-details/vertex-announces-program-updates-type-1-diabetes-portfolio (2025).

80. JDCA. Practical Cure Project Update: Beta-02 ßAir Bio-Artificial Pancreas. *Juvenile Diabetes Cure Alliance* 2–7 https://www.thejdca.org/publications/report-library/archived-reports/2017-reports/practical-cure-project-update-beta-02-air-bio-artificial-pancreas.html

(2017).

81. Carlsson, P. O. *et al.* Transplantation of macroencapsulated human islets within the bioartificial pancreas βAir to patients with type 1 diabetes mellitus. *Am. J. Transplant.* **18**, 1735–1744 (2018).

82. Candiello, J., Singh, S. S., Task, K., Kumta, P. N. & Banerjee, I. Early differentiation patterning of mouse embryonic stem cells in response to variations in alginate substrate stiffness. *J. Biol. Eng.* **7**, (2013).

83. Nyitray, C. E., Chavez, M. G. & Desai, T. A. Compliant 3D microenvironment improves β-cell cluster insulin expression through mechanosensing and β-catenin signaling. *Tissue Eng. - Part A* **20**, 1888–1895 (2014).

84. Hu, C. *et al.* Gelation behavior and mechanism of alginate with calcium: Dependence on monovalent counterions. *Carbohydr. Polym.* **294**, 119788 (2022).

85. Wilson, J., Najia, M. A., Saeed, R. & McDevitt, T. Alginate Encapsulation Parameters Influence the Differentiation of Microencapsulated Embryonic Stem Cell Aggregates. **111**, 618–631 (2014).

86. Oda, H., Konno, T. & Ishihara, K. Efficient differentiation of stem cells encapsulated in a cytocompatible phospholipid polymer hydrogel with tunable physical properties. *Biomaterials* **56**, 86–91 (2015).

87. Richardson, T., Barner, S., Candiello, J., Kumta, P. N. & Banerjee, I. Capsule stiffness regulates the efficiency of pancreatic differentiation of human embryonic stem cells. *Acta Biomater.* **35**, 153–165 (2016).

88. Mahaddalkar, P. U. *et al.* Generation of pancreatic β cells from CD177+ anterior definitive endoderm. *Nat. Biotechnol.* **38**, 1061–1072 (2020).

89. Brassard, J. A., Dharmaraj, S. S., Orimi, H. E. & Vdovenko, D. Iterative sacrificial 3D printing and polymer casting to create complex vascular grafts and multi-compartment bioartificial organs. (2024) doi:10.1101/2024.09.29.615298.

90. Shin, D. S. *et al.* Mesenchymal stromal cell encapsulation in uniform chitosan beads using microchannel emulsification. 1–22 (2022).

91. Kim, K., Cheng, J., Liu, Q., Wu, X. Y. & Sun, Y. Investigation of mechanical properties of soft hydrogel microcapsules in relation to protein delivery using a MEMS force sensor. *J. Biomed. Mater. Res. - Part A* **92**, 103–113 (2010).

92. Aigha, I. I. & Abdelalim, E. M. NKX6.1 transcription factor: a crucial regulator of pancreatic β cell development, identity, and proliferation. *Stem Cell Res. Ther.* **11**, 1–14 (2020).

93. Dang, T. *et al.* Computational fluid dynamic characterization of vertical-wheel bioreactors used for effective scale-up of human induced pluripotent stem cell aggregate culture. 1–18 (2021) doi:10.1002/cjce.24253.

94. Gao, T. *et al.* Pdx1 maintains β cell identity and function by repressing an α cell program. *Cell Metab.* **19**, 259–271 (2014).

95. Zhang, Y. *et al.* PDX-1: A Promising Therapeutic Target to Reverse Diabetes. *Biomolecules* **12**, (2022).

96. Davis, J. C. *et al.* Glucose Response by Stem Cell-Derived β Cells In Vitro Is Inhibited by

a Bottleneck in Glycolysis. **31**, (2020).

97. Rorsman, P. & Ashcroft, F. M. Pancreatic β-cell electrical activity and insulin secretion: Of mice and men. *Physiol. Rev.* **98**, 117–214 (2018).

98. McTaggart, J. S., Clark, R. H. & Ashcroft, F. M. The role of the KATP channel in glucose homeostasis in health and disease: More than meets the islet. *J. Physiol.* **588**, 3201–3209 (2010).

99. Bauwens, C. L. *et al.* Geometric control of cardiomyogenic induction in human pluripotent stem cells. *Tissue Eng. - Part A* **17**, 1901–1909 (2011).

100. Sart, S., Bejoy, J. & Li, Y. Characterization of 3D pluripotent stem cell aggregates and the impact of their properties on bioprocessing. *Process Biochem.* **59**, 276–288 (2017).

101. Bhujbal, S. V, Paredes-juarez, G. A. & Niclou, S. P. Factors in fl uencing the mechanical stability of alginate beads applicable for immunoisolation of mammalian cells. *J. Mech. Behav. Biomed. Mater.* **37**, 196–208 (2014).

102. Malandrino, A. *et al.* Plasticity of 3D Hydrogels Predicts Cell Biological Behavior. *Biomacromolecules* (2024) doi:10.1021/acs.biomac.4c00765.

103. Johnson, C. D., Aranda-Espinoza, H. & Fisher, J. P. A Case for Material Stiffness as a Design Parameter in Encapsulated Islet Transplantation. *Tissue Eng. - Part B Rev.* **29**, 334–346 (2023).

104. Kharbikar, B. N., Mohindra, P. & Desai, T. A. Review Biomaterials to enhance stem cell transplantation. *Stem Cell* **29**, 692–721 (2022).

105. Wang, N., Adams, G., Buttery, L., Falcone, F. H. & Stolnik, S. Alginate encapsulation

technology supports embryonic stem cells differentiation into insulin-producing cells. *J. Biotechnol.* **144**, 304–312 (2009).

106. Legøy, T. A. *et al.* Encapsulation boosts islet-cell signature in differentiating human induced pluripotent stem cells via integrin signalling. *Sci. Rep.* **10**, 1–16 (2020).

107. Bozza, A. *et al.* Biomaterials Neural differentiation of pluripotent cells in 3D alginate-based cultures. *Biomaterials* **35**, 4636–4645 (2014).

108. Tran, R., Moraes, C. & Hoesli, C. A. Developmentally-Inspired Biomimetic Culture Models to Produce Functional Islet-Like Cells From Pluripotent Precursors. *Front. Bioeng. Biotechnol.* **8**, 1–17 (2020).

109. Amin, L., Deng, K., Tran, H. A., Singh, R. & Rnjak-kovacina, J. Glucose-Dependent Insulin Secretion from β Cell Spheroids Is Enhanced by Embedding into Softer Alginate Hydrogels Functionalised with RGD Peptide. (2022).

110. Enck, K. *et al.* Effect of alginate matrix engineered to mimic the pancreatic microenvironment on encapsulated islet function. 1177–1185 (2021) doi:10.1002/bit.27641.

111. Peterson, Q. P. *et al.* A method for the generation of human stem cell-derived alpha cells. *Nat. Commun.* **11**, 1–14 (2020).

112. Ebrahim, N., Shakirova, K. & Dashinimaev, E. PDX1 is the cornerstone of pancreatic β-cell functions and identity. *Front. Mol. Biosci.* **9**, 1–18 (2022).

113. Hakim, F. *et al.* High Oxygen Condition Facilitates the Differentiation of Mouse and Human Pluripotent Stem Cells into Pancreatic Progenitors and Insulin-producing Cells *

□. **289**, 9623–9638 (2014).

114. Ilc, K., Mazure, N. M., Pouysse, J., Scharfmann, R. & Duvillie, B. Oxygen Tension Regulates Pancreatic ␍ -Cell Differentiation Through Hypoxia-Inducible Factor 1 ␣. **59**, (2010).

115. Nostro, M. C. *et al.* Stage-specific signaling through TGF b family members and WNT regulates patterning and pancreatic specification of human pluripotent stem cells. **1445**, 861–871 (2011).

116. CECHIN, S. *et al.* Influence of In Vitro and In Vivo Oxygen Modulation on b Cell Differentiation From Human Embryonic Stem Cells. 277–289 (2014).

117. Kropp, C. *et al.* Impact of Feeding Strategies on the Scalable Expansion of Human Pluripotent Stem Cells in Single-Use Stirred Tank Bioreactors. *Stem Cells Transl. Med.* **5**, 1289–1301 (2016).

Appendix

Table 2. Pancreatic differentiation protocol (based on previously publish protocols [44,47,53,88]

Differentiation Stage	Lineage	Basal Media	Basal Media Supplements (Final Concentration)	Growth Factors (Final Concentration)	Small Molecules (Final Concentration)
S0D0	Human Pluripotent Stem Cells	mTesR1	-	-	10 µM Y-27632
S0D1	Human Pluripotent Stem Cells	mTesR1	-	-	-
S1D1-S1D3	Definitive endoderm	MCDB 131	1X GlutaMAX 10mM D-(+)-Glucose 1.5 g/L Sodium Bicarbonate 0.5% FAF-BSA	0.1 µg/mL Activin A Protein	3 µM CHIR 99021 (S1D1 only)
S2D1-S2D3	Primitive gut tube	MCDB 131	1X GlutaMAX 10 mM D-(+)-Glucose 1.5 g/L Sodium Bicarbonate 0.5% FAF-BSA	50 ng/mL rh FGF-7, ACF	1.25 µM IWP-2 0.25 mM L-Ascorbic acid
S3D1-S3D2	Posterior Foregut	MCDB 131	1X GlutaMAX 15 mM D-(+)-Glucose 2.5 g/L Sodium Bicarbonate 2% FAF-BSA 0.25 mM L-Ascorbic acid 1X ITS-X	50 ng/mL rh FGF-7, ACF	0.2 µM TPB 0.25 µM SANT-1 1 µM Retinoic Acid 0.1 µM LDN193189

Differentiation Stage	Lineage	Basal Media	Basal Media Supplements (Final Concentration)	Growth Factors (Final Concentration)	Small Molecules (Final Concentration)
S4D1-S4D4	Pancreatic progenitor	MCDB 131	1X GlutaMAX 15 mM D-(+)-Glucose 2.5 g/L Sodium Bicarbonate 2% FAF-BSA 0.25 mM L-Ascorbic acid 1X ITS-X	50 ng/mL rh FGF-7, ACF	0.1 µM TPB 0.25 µM SANT-1 0.1 µM Retinoic Acid 0.2 µM LDN193189
S4D5 (Aggrewell Plates)	Pancreatic progenitor	MCDB 131	1X GlutaMAX 15 mM D-(+)-Glucose 2.5 g/L Sodium Bicarbonate 2% FAF-BSA 0.25 mM L-Ascorbic acid 1X ITS-X	50 ng/mL rh FGF-7, ACF	10 µM Y-27632 0.1 µM TPB 0.25 µM SANT-1 0.1 µM Retinoic Acid 0.2 µM LDN193189
S5D1-S5D5	Endocrine progenitor	MCDB 131	1X GlutaMAX 20 mM D-(+)-Glucose 1.5 g/L Sodium Bicarbonate 2% FAF-BSA 1X ITS-X 10 µg/mL Heparin 10 µM Zinc Sulfate 100 U/mL PenStrep	-	0.25 µM SANT-1 0.05 µM Retinoic Acid 0.1 µM LDN193189 0.1 µM γ-Secretase Inhibidor XX 10 µM Alk-5 inhibitor 1 µM T3

Differentiation Stage	Lineage	Basal Media	Basal Media Supplements (Final Concentration)	Growth Factors (Final Concentration)	Small Molecules (Final Concentration)
S6D1-S6D7	Immature SC-islets	MCDB 131	1X GlutaMAX 20 mM D-(+)-Glucose 1.5 g/L Sodium Bicarbonate 2% FAF-BSA 1X ITS-X 10 µg/mL Heparin 10 µM Zinc Sulfate 100 U/mL PenStrep	-	0.1 µM LDN193189 0.1 µM γ-Secretase Inhibitor XX 10µM Alk-5 inhibidor 1 µM T3
S7D1-D7D25	Maturing SC-islets	MCDB 131	1X GlutaMAX 1g/L Sodium Bicarbonate 2% FAF-BSA 1X ITS-X 10 µg/mL Heparin 10µM Zinc Sulfate 100 U/mL PenStrep 1X NEAA 1X Trace Elements A 1X Trace Elements B 1 mM N-Acetyl-L-cysteine	-	1 µM T3

Table 3. Catalog number and manufacturer of the basal media and supplements used in the pancreatic differentiation

Basal Media	Basal Media Supplements	Manufacturer	Catalog #
mTesR1	-	STEMCELL Technologies	85850
MCDB 131	-	Gibco™	10372019
-	GlutaMAX	Gibco™	35050061
-	D-(+)-Glucose	Sigma Aldrich	G8769
-	Sodium Bicarbonate	Thermo Fisher Scientific	S233-500
-	Fatty Acid Free-Bovine Serum Albumin (FAF-BSA)	PROLIANT Health & Biologicals	68700
-	Ascorbic acid	Sigma Aldrich	A4544
-	Insulin-Transferrin-Selenium-Ethanolamine (ITS-X)	Thermo Fisher Scientific	51500056
-	Heparin	Sigma Aldrich	H3149-100ku
-	Zinc Sulfate	Thermo Fisher Scientific	389802500
	Penicillin-Streptomycin (PenStrep)	Thermo Fisher Scientific	15140122
	Non-Essential Amino Acids (NEAA)	Gibco™	11140050
	Trace Elements A	Corning®	25-021-CI
	Trace Elements B	Corning®	25-022-CI
	N-Acetyl-L-cysteine (NAAC)	Sigma Aldrich	A9165

Table 4. Catalog number and manufacturer of the growth factors used in the pancreatic differentiation

Growth Factor or Small Molecule	Manufacturer	Catalog #
Y-27632	STEMCELL Technologies	72308
Activin A Protein	Cedarlane	338-AC-50/CF
CHIR 99021	Cedarlane	4423/10
rh FGF-7, ACF	Thermo Fisher Scientific	78186.2
IWP-2	Cedarlane	13951
Ascorbic acid	Sigma Aldrich	A4544
TPB	Sigma Aldrich	565740
SANT-1	Cedarlane	14933
Retinoic Acid	Sigma Aldrich	R2625
LDN193189	Sigma Aldrich	SML0559
Secretase Inhibitor XX	Sigma Aldrich	565789
Alk-5 inhibitor	Cedarlane	14794
3,3′,5-Triiodo-L-thyronine sodium salt (T3)	Sigma Aldrich	T6397

Table 5. Conjugated antibodies used in the Flow Cytometry analysis across various pancreatic differentiation stages

Pancreatic Differentiation Stage	Lineage	Antibody	Vendor & Catalog #
Stage 1 Day 3	Definitive endoderm	SOX17-PE	BD Biosciences/561591
		PE mouse IgG1	BD Biosciences/554680
Stage 4 Day 3	Pancreatic progenitor	PDX1-PE	BD Biosciences/562161
		NKX6.1-AF647	BD Biosciences/563338
		NEUROD1-PE	BD Biosciences/563001
		PE mouse IgG1	BD Biosciences/554680
		AlexaFluor® 647 mouse IgG1	BD Biosciences/557732
Stage 7 Day 10 & 25	Maturing SC-islets	PDX1-PE	BD Biosciences/562161
		NKX6.1-AF647	BD Biosciences/563338
		NEUROD1-PE	BD Biosciences/563001
		Glucagon-PE	BD Biosciences/565860
		C-peptide-AF647	BD Biosciences/565831
		PE mouse IgG1	BD Biosciences/554680
		AlexaFluor® 647 mouse IgG1	BD Biosciences/557732